ANHYDRITE DEPOSITION IN CAWAYAN WELLS, BACMAN GEOTHERMAL FIELD, PHILIPPINES: PREDICTION AND POSSIBLE REMEDIES

Fidel S. See
Geothermal Division, Geoscientific Dept.
PNOC-Energy Development Corporation
PNPC Complex Memtt Road. Ft. Bonifacio.
Makati, Meuo Manila.
PHILIPPINES

ABSTRACT

The anhydrite mineral deposition inside the wellbores of Cawayan wells is investigated in order to predict its occurrence and come up with possible remedies. The chemistry of the fluids is thoroughly evaiuared and some geochemical indicators of deposition such as Ca^{++}, SO_4^{--}, Mg^{++}, SiO_2, and Cl^- are established. The behaviour of various calcium and sulfate species during deposition, and the effects of, temperature and pH are determined using the SOLVEQ and WATCH 2.1 programs. Results show that at higher temperatures. sulfate and calcium species decrease in activity and this tends to increase supersaturation. At lower pH, sulfate activity is significantly reduced by the formation of bisulfate ions, and undersaturation is attained; at higher pH, undersaturation also occurs due to decrease in calcium activity. However, calcite supersaturates at higher pH. The CHILLER program is utilized to simulate fluid-fluid mixing, and determine the effects of NaCl addition, Na_2HPO_4 addition, acid treatment, and CaCl, injection on anhydrite deposition. Results show that NaCI, Na_2HPO_4 and HCl are possible inhibitors of anhydrite deposition. Increasing the salinity of production fluid before mixing with high-sulfate waters tends to retard deposition and increase the amount of mixing fluid necessary to initiate formation of anhydrite. Na_2HPO_4 prevents anhydrire deposition by significantly reducing activity of calcium through association with phosphate ions. However, the solution tends to become supersaturated with respect to apatite. CaCI, addition can induce deposition in the acid zones but this further lowers the pH of the hi&-sulfate acid fluid as bisulfate dissociates into sulfare ions and releases hydrogen ions.

10 INTRODUCTION

The Bacman geothermal production field is located on the southern tip of the Bicol peninsula in the Philippines. A 110 MWe geothermal power plant in the Palayan Bayan sector: and a 20 MWe modular plant in the Cawayan sector have been fully operational since 1994. A second 20 MWe plant is currently under development in the Botong sector (Figure 1).

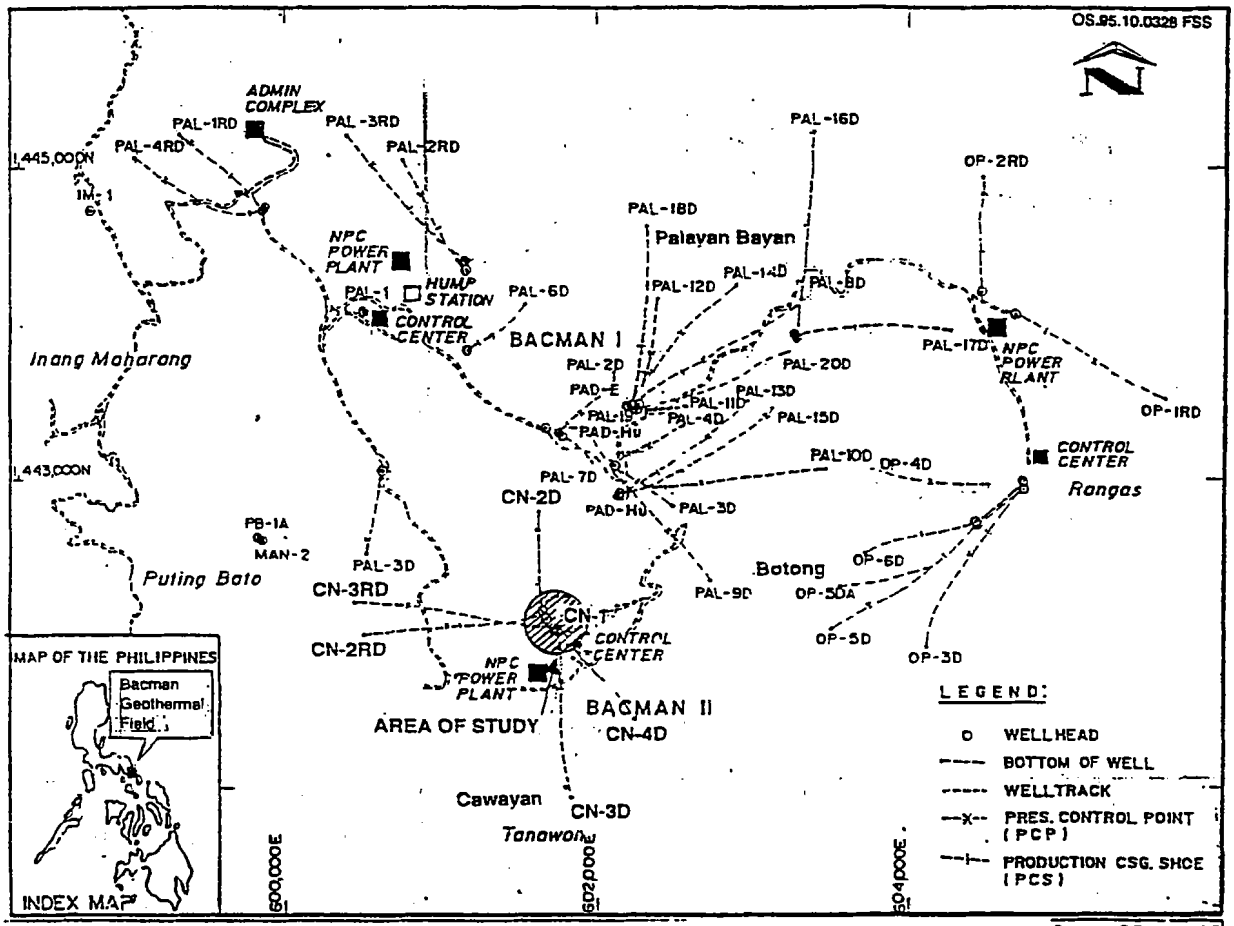

FIGURE 1: Location map of Bacman geothermal field and well targets

The Cawayan sector is initially composed of two production wells, each with an output of about ten megawatts. Less than a year after commissioning, problems associated with corrosion and mineral deposition inside the wellbores started to significantly decrease the output of the two wells. Petrological analyses of the mineral deposits yielded mostly anhydrite. with small amounts of pyrite, opaques. and corrosion products. Work-over operations using drilling rigs were conducted to mechanically clean the boreholes. The improvement after cleaning was however only temporary and after a few months, deposition started to clog the wells again. Subsequently two additional wells were drilled to maintain the 20 MWe production of the field. Mitigating measures undertaken (Fragata, 1994) in the new wells are: deepening the production casing shoes, casing-off and cementing acid zones, and using corrosion-resistant casings. Calcium chloride injection in the acid zones is also practised during drilling.

Despite the preventive measures implemented, the possibility of anhydrite and other mineral deposition during long-term production cannot be totally eliminated. The original wells, on the other hand are still hampered by anhydrite deposition and regular cleaning by drilling rigs is very costly. Therefore a more thorough understanding of the deposition process, an efficient and reliable method of monitoring, and

investigation of possible methods of deposition control, are necessary.

The aim with this report is to determine the anhydrite saturation conditions of the Cawayan fluids; establish some geochemical indicators of anhydrite deposition; characterize speciation and mineral-solution equilibria of the fluids responsible for the deposition; simulate saturation conditions at different temperatures, pH, salinity, and mixing proportions; and investigate possible chemical methods of control through simulations.

2.0 BACKGROUND

2.1 Geology and hydrothermal alteration

The Cawayan wells penetrated the so-called Pocdol volcanic formation, one of the lithologic units of the Bacman geothermal field. This formation is composed of moderately to intensely and completely altered voicanic rocks of andesite lavas. tuffs, ana breccia (PNOC-EDC, 1989). This is dissected by the Gayong sedimentary formation in the Botong and Palayan Bayan sectors. and by several andesitic and microdioritic dykes called the Cawayan intrusive compiex (PNOC-EDC. 1989). All the Cawayan wells. except CN-3D intersected the Cawayan intrusive complex (Fragata 1991). The hydrothermal alteration encountered. in the wells is generally neutral.. These consist of quam. calcite. anhydrite, epidote, illite, smecrite, actinolite, biotite, chlorite, clinozoisite, pyrite, hematite. magnetite, and goethite (Ramos. 1991). Acid alteration products consisting of kaolinite, dickite. alunite. and pyrophyllite, are also abundant: sulfur crystals have been observed megascopically in well CN-2RD at 100-415 mMD (Ramos. I991). Acid alteration is usually observed at shallower depths. above 1000 mVD. but has also been detected at deeper levels such as diaspore at 1710 mVD in well CN-2RD (Ramos. 1991).

2.2 Fluid chemistry

The chemistry of the Cawayan fluids has been discussed thoroughly in several PNOC-EDC internal reports (e.g. KRTA (1985); Solis (1 988); See (1991)). There are generally two types of thermal fluids in the sector. First the dominant fluid which is the honer and deeper, neutral geothermal production brine; and the second one is the colder, shallower, high-sulfate and usually acidic fluid. Particular interest has been devoted to the occurrence and origin of the acid fluids in the area.

The production fluids are neutral geothermal brines with baseline sulfate concentrations of 19 to *29* mg/kg, and calcium concentrations of 138 to 175 mg/kg in weirbox and Webre separator samples. The weirbox samples are coilected at atmospheric pressure while Webre samples are collected at 5 to 8.5 bars absolute. The fluids are relatively saline with chloride concentrations of approximately 7000 to 8000 mg/kg and ionic strength of about *0.2000* in water phase. pH measured at 25°C ranges from 7.05 to 7.83. Quartz and measured temperatures range from 270 to 275°C.

In contrast the acid fluids have been found to be more dilute, colder, and contain enormous amounts of sulfate ranging from 381 to 1630 mg/kg. pH measured at 25°C ranges from *2.6* to 5.1. Calcium is relativeiy iow with concentrations that range from *6* to 89 mg/kg. Chloride concentrations vary from 142 to 5000 mg/kg, and the ionic strength is less than 0.1 000. Silica quartz geothermometer and measured temperatures range from 230°C to approximately *260°C.* These fluids are also characterized by high iron and magnesium contents. In Cawayan production wells, these types of fluid are normally found in the shallower zones, from about 1000 mVD and above. However, in reinjection wells such as CN-2RD and CN-3RD, high-sulfate fluids exist at depth.

Representative chemical data used in this study are presented in Tables 1 and 2.

2 3 Blockage history and mineral composition

As early as 1983, a blockage inside the wellbore of CN-1 was detected. The initial blockage, consisting of 90% corrosion producrs and 10% anhydrite, was found in this well at 1599 m VD on May 11, 1983. A subsequent survey in May 1984 located the blockage at 1593 m VD. and then it apparently extended to 1598 m VD where it was detected in September 1984. Scraper samples yielded corrosion products (40%), cuttings (30%), calcite (20%), and anhydrite (10%) . In February 1990, the obstruction was detected at 1383 m VD and the composition was determined to be mainly anhydrite (46%) with significant amounts of opaques, vermiculite, cuttings, and carbonates. The well was then cleaned by a drilling rig prior to commissioning. During the production stage, wellhead pressure started to decline and a second rig cleaning was carried out. Deposition however continued to take place. During the latest survey conducted in May 1994, the blockage was detected at 1019 m VD and the composition was mostly anhydrite (76%) with corrosion products and some cement and formation rock indicating casing corrosion.

In well CN-3D. the blockage was detected at 1076 m VD in November 1994. when the well was on-line to the power plant. The deposits were composed of 90% anhydrite and 10% pyrite. In July 1995. the blockage extended up to 886 m VD and the output of the well declined significantly.
Details of petrological analyses of the minerals collected from the wellbores are shown in Table 3.

3.0 DESCRIPTION OF PRESENT WORK

This study is essentially a detailed analytical evaluation of chemical data from wells in which anhydrire deposition has taken place. utilizing speciation and reaction path programs. Saturation conditions of the fluids with respect to anhydrite are determined using the speciation programs WATCH 2.1 (Amorsson. et al., 1982; Bjarnason, 1994) and SOLVEQ (Reed and Spycher. 1990a). Simulation runs varying parameters such as pH. and temperature are conducted to determine how the fluid chemistry will change especially with respect to anhydrite saturation. The reaction path program CHILLER (Reed and Spycner, 1992) is used to simulate fluid-fluid mixing of neutral geothermal brine and high-sulfate acid downhole fluid. simuiate the effect of sodium chloride addition on anhydrite deposition, and evaluate the effect of CaCI, injection in the acid zones. The changes with time of the concentration of several chemical parameters are evaluated as indicators of deposition. Speciation of various calcium and sulfate species fiom simulation runs are closely examined in order to find out the behaviour of these species and their effects on anhydrite saturation at different conditions. The CHILLER program is also used to simulate the effects of NaCl. Na_2HPO_4 and HCI as possible inhibitors of anhydrite deposition.

4.0 REVIEW

4.1 Literature review

A great deal of experimental work on the solubility of anhyarite has been described, the most notable being that of Dickson, et al. (1963); Blount and Dickson (1969); and Yeatts and Marshall (1969). Dickson, et al. (1963) determined the rapid decrease of anhydrite solubility in pure water with increasing temperature at constant pressure. Blount and Dickson (1969), studied the decrease of anhydrite

solubility at different concentrations of $NaCl$-H_2O solutions with temperature at constant and variable pressures. It can be concluded on the basis of their experimental results that the solubiiity of anhydrite is generally controlled by temperature, pressure, and salinity. Using their experimental data from solubility studies, Dickson, et al., (1963) and Blount and Dickson, (1969), deduced that in natural hydrothermal' processes, anhydrite deposition can occur at the following conditions: migration of saturated solutions at constant temperature from rocks interstices governed by lithostatic pressure to fissures controlled by hydrostatic pressures; descent of saturated groundwater to hotter regions: and deposition in the pores of sedimentary rocks as a result of increase in temperature accompanying burial of accumulating sediments, from interstitial waters containing $CaSO_4$ originally entrapped during sedimentation. Direct precipitation from sea water is also a possibility as in the Svartsengi wells in Iceland where there is geochemical evidence of seawater intrusion and anhydrite deposition along structures (Bjamason, **J.O.,** pers. comm.). In the oil fields. the occurrence of calcium sulfate scale, mostly gypsum. in equipment and formation has been reponed by Vetter and Phillips (1970). Several other studies of anhydrire solubility are discussed and summarized in KRTA (1983). Mosr of the work done in that report is based on experimental conditions different from a geothermal chemical matrix.

In geothermal utilization, the occurrence of significant annydrire deposits in wellbores has not been much reponed. possibly because of the rarity of such cases. Its impact on geothermal development cannot. however. be underestimated as can be seen from the case ofthe Cawayan wells.

Several formulas for calculating the solubility and equiiibrium constants of anhydrite have been derived by various authors. Some are based on experimental results (e.g. Blount and Dickson. 1969) while others are calculated from thermodynamic data. 'A selection of equarions that may be applicable to geothermal fluid is presented in Appendix 1.

4.2 Saturation calculation

The dissolution-precipitation reaction of anhydrite can be expressed as.

$$CaSO_{4\,(s)} \rightleftharpoons Ca^{++}_{(aq)} + SO_4^{--}{}_{(aq)} \qquad (1)$$

and the reaction quotient is defined by,

$$Q = (a_{Ca^{++}} * a_{SO4^{--}}) / a_{CaSO4} \qquad (2)$$

where a is activity and unity for pure solid minerals like anhydrite. As with any chemical reaction, this either absorbs or releases energy which is the Gibbs free energy of reaction expressed as,

$$\Delta Gr = \Delta Gr^\circ + RT \ln Q \qquad (3)$$

where R is gas constant, T is absolute temperature, and ΔGr° is the standard Gibbs free energy usually given in the literature at 25°C and 1 bar. ΔGr° can be calculated at different temperatures based on available thermodynamic data on Cp (heat capacity), ΔHr° (heat of reaction), and S° (entropy), using established thermodynamic relationships. ΔGr° is defined as,

$$\Delta Gr^\circ = RT \ln K \qquad (4)$$

where Kis the thermodynamic equilibrium constant. At or near equilibrium conditions (i.e. no flow of energy is taking place), $\Delta Gr = 0$, thus equation (3) becomes,

$$\Delta Gr^\circ = -RT \ln Q \qquad (5)$$

and substituting equation (4)into this yields,

$$RT \ln K = -RT \ln Q \qquad (6)$$

Q can be calculated from laboratory analysis of calcium and sulfate speciated at desired temperature, using equation (2), while K is calculated from $\Delta Gr°$ using equation **(3).** So, basically the determination of saturation conditions is just a comparison between log K and log Q values. When log Q exceeds log K (which defines the amount of Ca^{++} and SO_4^{-} ions a solution can hold at a given temperature in a thermodynamic equilibrium system), supersaturation occurs and deposition may take place.

Anhydrite saturation is therefore governed by the activity of sulfate and calcium. but the activity of these two ions is affected by several factors such **as** pH, temperature, chemical mamx of the solution, **and** pressure.

5.0 **DEPOSITION** PARAMETERS

5.1 Evaluation of different formulas

Speciation programs such **as** WATCH and SOLVEQ can perform iterations to solve for mass-balance and chemical equilibrium equations. and compute for activities. speciation. log Ks and mineral saturation at different temperatures. However their application is nor always straightforward due to some limitations to equilibrium computations (Nordsrrom and Munoz, 1986). Validation by petrological analysis is helpful especially in cases where deposition samples can be obtained such **as** in the Cawayan wells. And thus in futurereplicationsthey can be used in monitoring with more certainty.

Several equations for computing anhydrite solubility are evaluated for comparison. Four equations yielded results that are comparable. Figure **2** shows the equilibrium curves obtained from the different equations. The calculations by Arnorsson, et al. (1982), and Reed and Spycher (1990a) are incorporated in the speciation programs used in this study. Computations of their log K values for anhydrite are mostly based on thermodynamic data by Helgeson (1969). Significant deviations of the two curves from each other **are** observed above 200°C, possibly because of the unreliability of some thermodynamic **data** above this temperature (Amonson, et al., 1982), resulting in discrepancy in the calculated log K values. The two **equations are validated using well samples collected during anhydrite deposition.** Both equations **show** supersaturation conditions during **the** deposition process with results from WATCH yielding a'higher degree of supersaturation.

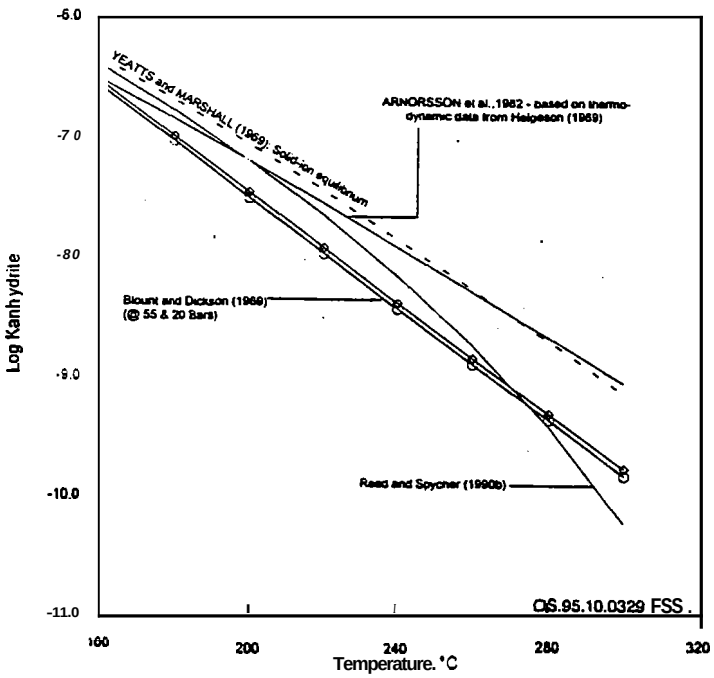

FIGURE 2: Comparison of equilibrium **curves** based **on** several formulas for calculating anhydrite solubiiity derived by various authors.

Blount and Dickson's (1969) equation is based on experimental data from H_2O and H_2O-NaCl solutions, and pressure effect is incorporated. ***This*** equation yielded relatively low values of log K at lower temperatures, but at higher temperatures the results were similar to those of **Reed** and Spycher (1990b).

Yeatts and Marshall's (1969) equation is based on solid-ion equilibrium and the calculated equilibrium curve is almost identical to that of Arnorsson, et al. (1982).

The different log K values calculated using the various equations are given in Table 4. The values are significantly different especially at temperatures above 200°C. But in application, they yielded similar saruration conditions.

5.2 Saturation conditions and mineral-solution equilibria

The saturation conditions of the Cawayan fluids with respecr to anhydrite during baseline and production stages are determined using both the WATCH and the SOLVEQ programs. Results in Figures 3a and b show that fluids from production wells (CN-1/CN-3D/CN-4D) are initially saturared (or slightly

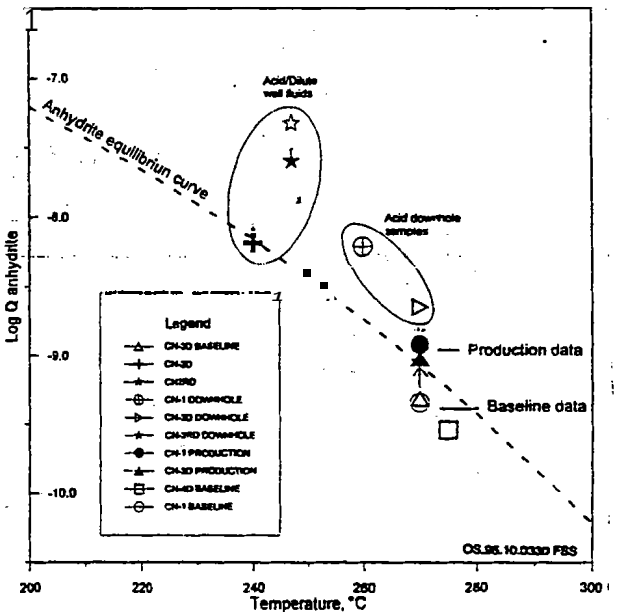

FIGURE 3a: Anhydrite saruration of Cawayan well fluids (baseline and production data) using the. SOLVEQ program by Reed and Spycher (1990a)

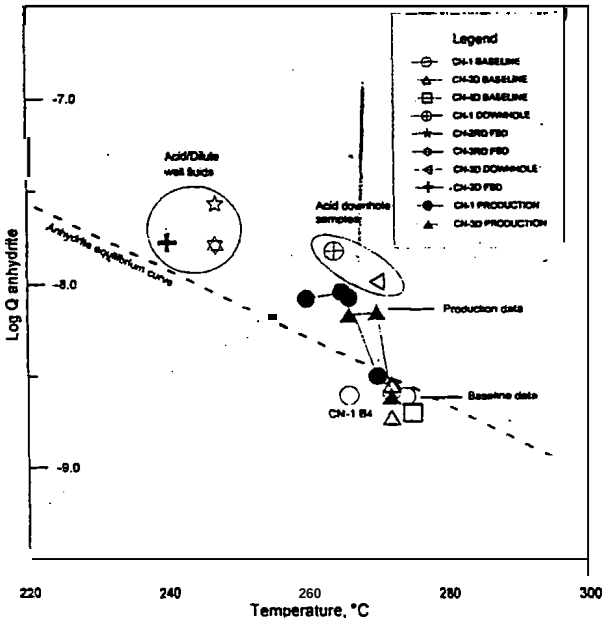

FIGURE 3b: Anhydrite saturation of Cawayan well fluids (baseline and production data) using the WATCH program by Amorsson, et al. (1982).

undersaturated) **with** anhydrite, suggesting **near** equilibrium with **this** mineral. During the production stage, data points from the producing wells CN-1 and CN-3D plotted above the anhydrite equilibrium curve suggesting that the fluids have become supersarurated **with** respect to anhydrite. Correspondingly, some geochemical parameters started to exhibit specific trends with time, **and** months later, the wellhead pressures started to decline. These results show that both speciation programs are sensitive to anhydrite saturation changes and can be effectively used for monitoring critical wells.

The acid and dilute fluids in the reinjection wells CN-2RD and CN-3RD, and the downhoie samples **from** CN-1 and CN-3D *are* all supersaturated with respect to anhydrite (Figures 3a **and** b). Evaluation of fluid equilibria **from** SOLVEQ runs, with some minerais identified from petrological anaiysis showed apparent equilibrium only **with** quartz (Figure **4).** The curves did not exhibit any common point of intersection along the log (Q/K)=0 line indicating that these fluids have not attained equilibrium with the identified minerais except quartz. The acid well fluids are also supersaturated wirh iron minerals suchas pyrite, and hematite because of elevated concentrations of iron, probably derived **from** dissolution of casing. CN-3RD which is slightly alkaline despite its high sulfate concentration and

proximity *to* the acid wells, is also supersaturated with respect to carbonate minerals such as dolomite, $CaMg(CO_3)_2$, and calcite suggesting the occurrence of high CO_2 concentrations in the well fluid. For anhydrite, all well fluids, except CN-2D, plotted above the equiiibrium line suggesting that this mineral is in excess in the solutions. The presence of sulfate-bearing minerals such as anhydrite and alunite, $KAl_3(OH)_6(SO_4)_2$ in the formation rocks of the wells is an indication of possibie precipitation of anhydrite from the fluid, and interaction with the rocks. However further investigation of fluid equilibria with other key and associated minerals found in the wells is necessary before this can be established.

The high-sulfare acid fluids in Bacman have been interpreted to have originated from the oxidation of H_2S in the vadose zone, and subsequently percolated to deeper levels (Solis et al., 1994). The results of sulfur and oxygen isotope analyses support this postulate. These fluids are believed to be the main source of excessive amounts of sulfate and the major cause of anhydrite deposition in the Cawayan wells.

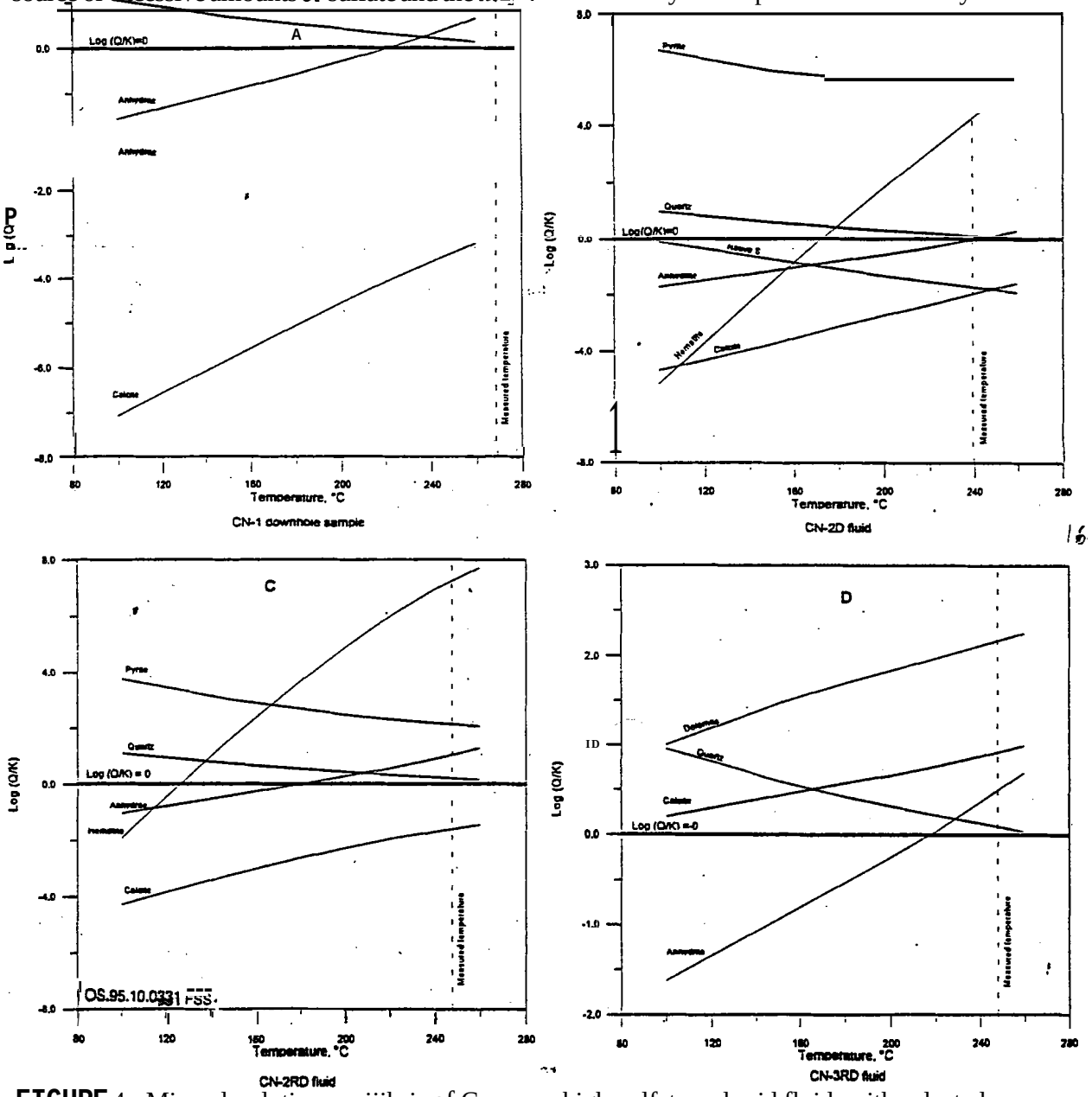

FIGURE 4: Mineral-solution equiiibria of Cawayan high-sulfate and acid fluids with selected minerals identified from petrological analysis; **A)** CN-1 downhole sample; B) CN-2D fluid; C) CN-2RD fluid. D) CN-3RD **fluid**

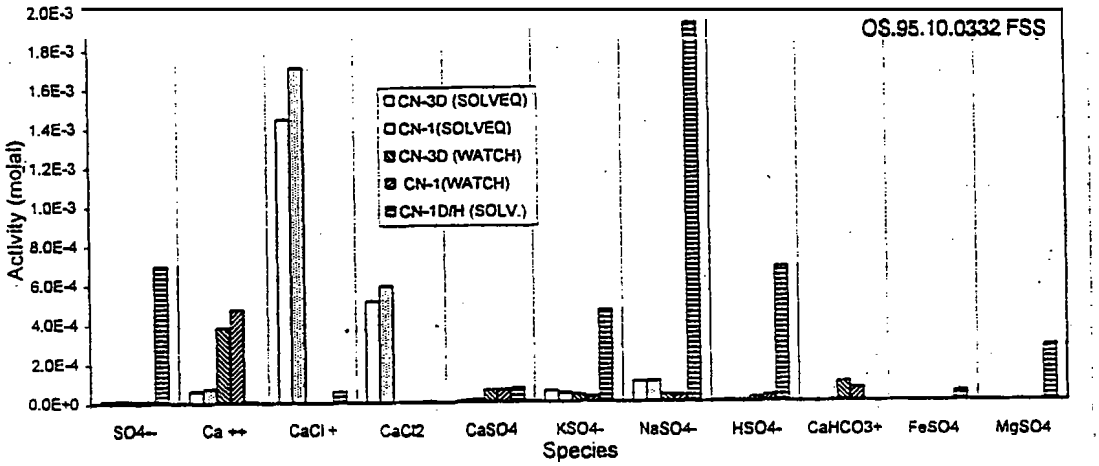

FIGURE 5: Calcium and sulfate species distribution of CN-1 and CN-3D supersaturated fluids. and , CN-1 high-sulfate acid downhole water at 270°C.

showed thar at 270°C, about 64% exist as CaCl', 23% as $CaCl_2$, 5% as $NaSO_4^-$, 3% as KSO_4; 3% as Ca^{++}, and 1% as SO; According to the results of WATCH in which the $CaCl^+$ and CaCl, species are not incorporated, the major ion is Ca^{++} at 57% while SO_4^{--} accounts for only 2%. Results of the SOLVEQ run show that the calcium-ions prefer association with chloride ions. while sulfare is more associated with sodium and potassium ions. The "free" calcium and sulfate ions that are directly involved in anhydrite deposition account for very small percentages of the coral species. These amounts are however sufficient to cause significant deposition. Sample calculations for CN-3D data show that an increase of a mere 1.02E-06 in molal activity (–i mg/kg increase in reservoir sulfate concentration) can lead to supersaturation. This shows that for initially saturated fluids. a very slight increase in sulfate or calcium activity can cause supersamration and possibly deposition. Temperature has also significant effects on the activity of caicium and sulfate species and this is discussed in Chapter 7.3.

For the downhole high-sulfate acid fluid speciation results show a different distribution at 270°C. The dominant species are $NaSO_4^-$ (44.9%), SO_4^{--} (16.4%), HSO_4^- (16.1%), and KSO_4^- (11.0%). Other sulfate forms practically absent from the production brine, such as $FeSO_4$ and $MgSO_4$ also exist because of the relatively high concentrations of iron and magnesium. These results reveal the source of high suifate ion activity responsible for the anhydrite deposition. However, despite the very high suifate concentration, its activity does not make it the dominant species. This implies that if sulfate association with sodium, potassium, magnesium, iron, and hydronium ions can be increased, the tendency for the fluid to deposit anhydrite can be reduced.

5.4 Geochemical indicators of anhydrite deposition

Evaluation of the chemistry of the Cawayan fluids before and during anhydrite deposition yielded chemical parameters that exhibited specific trends with time and may thus be useful as indicators. These parameters are sulfate, calcium, magnesium, chloride. and silica. A decrease in pH was also detected, but it is not very pronounced and exhibited an erratic trend. These chemical parameters already exhibit

unusual trends long before physical changes in the wells such as wellhead pressure (Figure *6)* and output decline become measurable. Data used in the plots covered a period of about fifteen months from baseline to production stages..

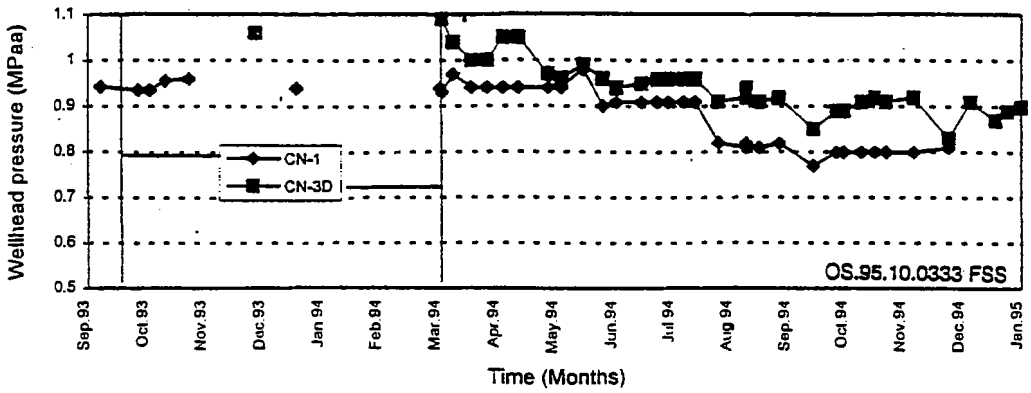

FIGURE 6: Wellhead pressure with time during anhydrite deposition. Vertical lines indicate the start of anhydrite supersaturation in CN-1 and CN-3D fluids.

Sulfate

Figure 7 shows the sulfate concentration trend with time. Suifare exhibited an increase during deposition. Its Concentration increased from **23** mg/kg (baseline saturation concentration) to 71 mg/kg for CN-1, and from **21** mg/kg to *66* mgkg for CN-**3D.** The increase in sulfate indicates the inflow of the mixing fluid identified at the upper horizon of the wells during downhole sampling. These fluids have earlier been characterized to be acid **and** contain high sulfate **ranging from** 810-975 mg/kg for CN-I and **62-96 mg/kg** for CN-3D. Sulfate appears to be a sensitive indicator of anhydrite deposition, increasing abruptly as supersaturation occurs and then exhibiting a steady increase throughout the deposition process suggesting a continuous influx of the mixing fluid.

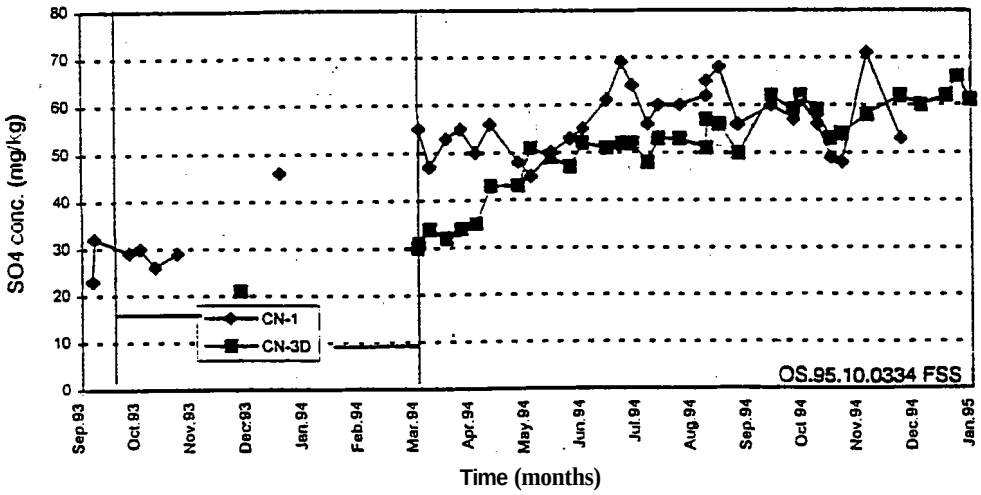

FIGURE 7: Sulfate concentration with time during anhydrite deposition. Vertical **lines** indicate start of anhydrite supersaturation for CN-1 and **CN-3D** fluids.

Calcium

Calcium initially exhibired **an** increase in concentration during **the** early stage of supersaturation (Figure **S), then** decreased abruptly and maintained a **steady** decline **as** deposition proceeded. Calcium concentration at the wellhead decreased gradually **from** about **196** mgkg to **146** mgkg in CN-I, and 180 mg/kg to 120 mg/kg in CN-3D. Since the mixing fluid is depleted in calcium, the calcium from the production brine is continuously being consumed by the excess sulfate during the formation of anhydrite.

Significant fluctuations **are** also observed especially for CN-1 indicating possible fluctuations in the rate

or amount being deposited. The decreasing trend however, is an indication that the rate of deposirion is increasing, probably because of the increasing acid-sulfate fluid influx.

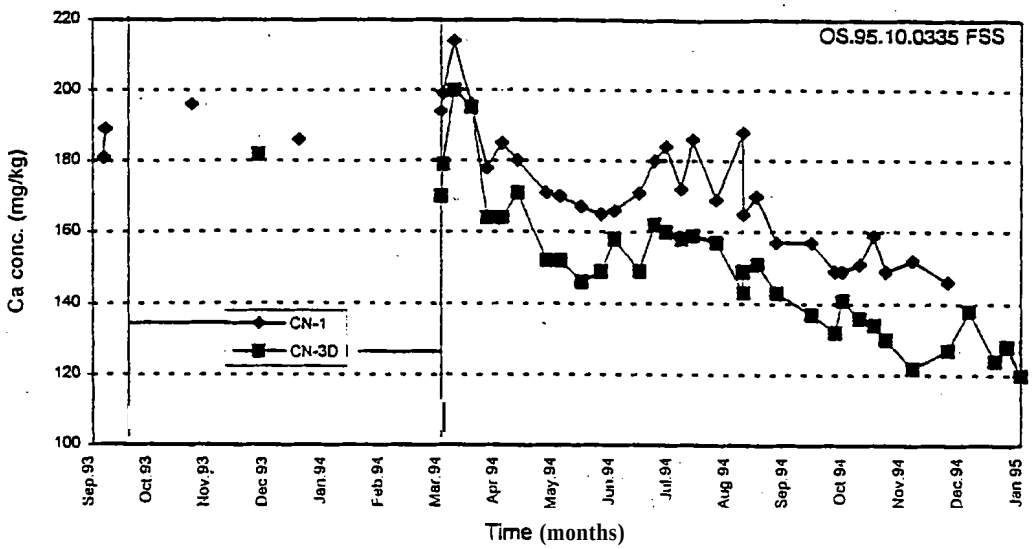

FIGURE 8: Calcium concentration with time during anhydrite deposition. Vertical lines indicate start of anhydrite supersaturation for CN-I and CN-3D.

Magnesium, chloride, and silica

Figures 9, 10. and 11 show the magnesium, chloride, and silica concentration trends with time. Although not directly involved in anhydrire deposition. in Cawayan wells. these chemical parameters are indicators of the relatively cold and dilute acid fluids that mix with the brine. The magnesium concentration increased. especially during the later part of deposition. suggesting the presence of a colder fluid. Chloride concentration **on** the other hand decreased. also showing the influx of the dilute fluid. Silica concentration similarly decreased especially in CN-1 indicating that the well is cooling down because of the influx of the colder mixing fluid. Silica however did not respond immediately and began to decrease only during the later stages of the deposirion process. In CN-3D, the drop in silica is not **as** pronounced. possibly because of a lesser amount of mixing fluid.

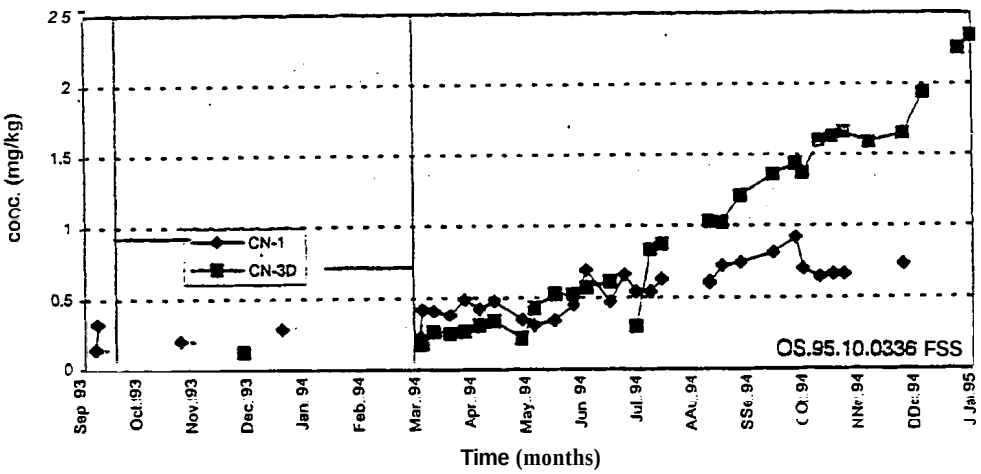

FIGURE 9: Magnesium concentration with time during anhydrite deposition. Vertical lines indicate **start** of anhydrite supersaturation for CN-I and CN-3D

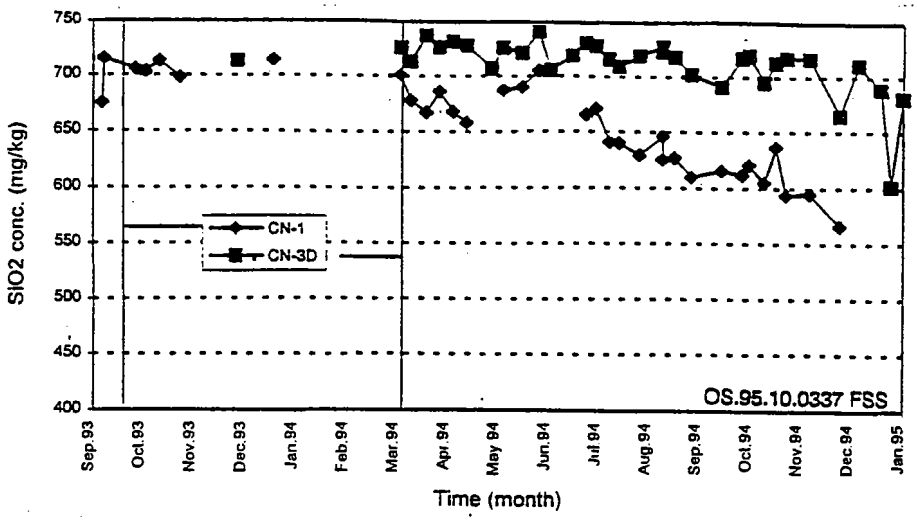

FIGURE 10: Silica concentration with time during anhydrite deposition. Vertical lines indicate start of anhydrite supersaturation for CN-1 and CN-3D.

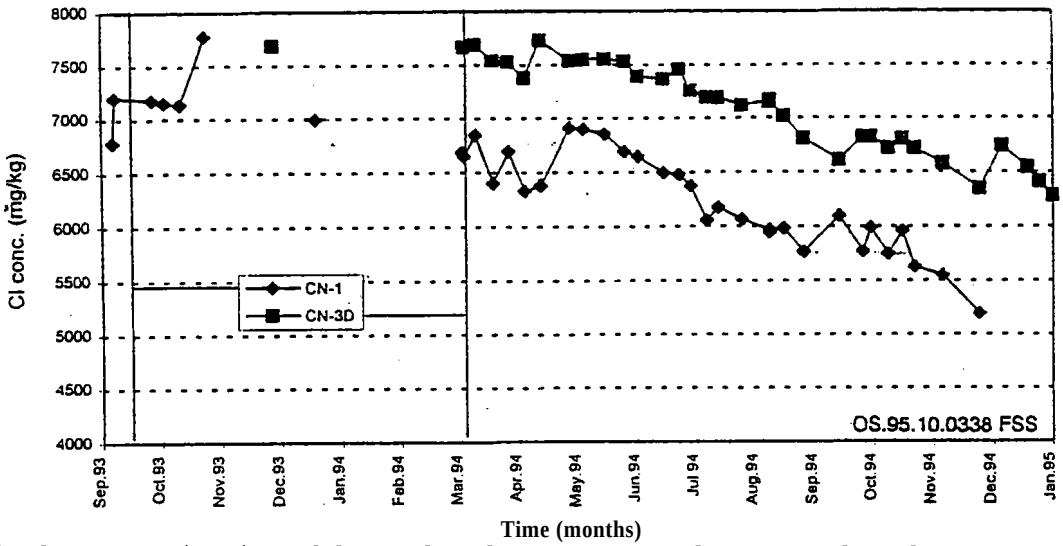

FIGURE 1: Chloride concenrration with time during anhydrite deposition. Vertical lines indicate start of anhydrite supersaturation for CN-I and CN-3D.

All these geochemical indicators continued to exhibit trends. either increasing or decreasing, throughout the deposition process with no indications of levelling-off or attainment of constant values. These results suggest that the influx of mixing fluids in the wells increases continuously and the rate of deposition is also increasing.

6.0 MIXING SIMULATIONS

The anhydrite deposits in the Cawayan wells have been deduced to be the end-product of mixing of high-sulfate acid fluids and calcium-rich geothermal brine. The baseline and production anhydrite saturation conditions, downhole chemistry, and the trends exhibited by the geochemical indicators support this conclusion.

Reaction path programs can provide information about the resultant mineral composition and aqueous-speciation for a given set of initial conditions and a given set of hypothetical reactions (Nordstrom and Munoz, 1986). The CHILLER program (Reed and Spycher, 1992) is a reaction path program that can simulate the addition or mixing of an aqueous solution, solids, or gases to an existing solution at different temperatures and mixing fractions. Most minerals and equiiibrium reactions of species found in typical geothermal fluids are incorporated in this program through its aatabase SOLTHERM (Reed and Spycher, 1990b). The "coolbrew" option of the program is used to simulate fluid-fluid mixing of the Cawayan production fluid and the high-sulfate acid downhole water from CN-1 and CN-3D, at

different temperatures. Application in this particular case is faciiitated by the petrological analysis results for the deposits inside the wellbores; minerals nor found are "suppressed", avoiding unnecessary equilibrations and thus computing time is faster and simulations more accurate. Mineral suppression is commonly used to disallow kinetically disfavored minerals, seiecred on the judgement of the user (Reed and Spycher, 1992). Minerals suppressed in this run and the succeeding runs include quartz, chalcedony, talc, tremolite, and diopside. These minerals have been calculated by CHILLER as supersaturated, but were not detected by petrological analysis at any given time. Therefore, the suppression of these minerals has a sound basis.

Figure 12 shows the results of mixing simulations. Mixing is carried out by titrating a kilogram of the baseline water sample with 0.01 to 0.10 fractions of downhole water at 270, 260. and 200°C. For CN-1, the downhole mixing fluid is collected at 1150 mVD (near the depth of deposition) with pH 3.2 and contains 884 mg/kg sulfate. Originally, the CN-1 production fluid is just saturated with anhydrite (Figures 3a and b) with no deposition taking place. As mixing with the acid downhoie fluid starts. sulfate activity begins to increase. At the 270 °C mixing temperature. deposition starts when the fraction of the downhole fluid is 0.03, with approximately 2.1E-03 g of anhydrite forming. From this point, the amount of anhydrite deposited increases significantly with the amount of mixing fluid addea. Calcium activity started to decrease as anhydrite formed while sulfare continued to increase because of the additional sulfate from the mixing fluid. The increase in sulfate activity is, however, not proportional to the increase in the fraction of mixing fluid added because it is to some extent consumed by anhydrite.. Such behavior of these *two* species is reflected in the calcium and sulfate concentrations of the wellhead samples and plotted in Figures 7 & 8 as geochemical indicators. The hydrogen ion (H^+) activity also exhibired slight increases due to the acidity of the mixing fluid. Decrease in pH has also been measured at the surface. Finally, for a mixing fluid fraction of 0.10 (or 10%), the amount ofanhydrite deposited is estimated at 7.0E-02 g. The downhole pH decreases from 6.61 to 5.62, calcium acivity drops from 6.02E-05 to 5.0E-05 molal. and sulfate activity increased from 7.45E-06 to 1.63E-05 molal. Hematite deposits also formed because ofthe high iron content of the mixing fluid. The amount of hematite however is small compared with that of anhydrite. Simulations at mixing fluid temperatures of 260°C and 200°C yielded similar results but smaller amount'of anhydrite deposits, and deposition starts at a mixing fraction of 0.04. This simulation result from CN-I agrees with previous evidence that mixing of the two different fluids is the cause of anhydrite deposition. and validates the thermodynamic conditions in the program for this case. The results can also be used (if properly calibrated with pemnent data such as flowrate, casing volume and the results of caliper or go-devil

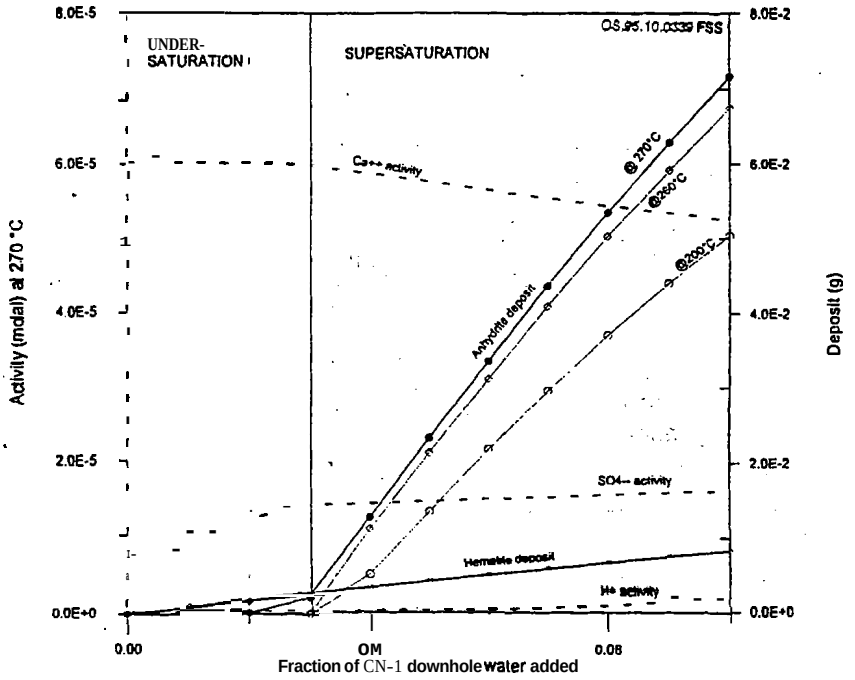

FIGURE 12: Simulated mixing of CN-1 production fluid and acidic high-sulfate downhole water at different temperarures. Mixing simulation performed using the **CHILLER** program. At 270°C deposition srarts at mixing fraction 0.03. At 260 and 200°C deposition occurs at fraction 0.04. Hematite is also deposited.

surveys) to estimare the volume of deposits formed and thus might be useful in predicting how long a well can produce before cleaning operations are scheduled.

The results of a similar simulation with CN-3D fluids did not yield supersaturation probably because of the much lower sulfate concentration of the mixing fluid used (96 mg/kg). The deposition in CN-3D, however, indicates that a more sulfate-rich fluid is mixing with the production brine.

7.0 SATURATION CHANGES AT DIFFERENT CONDITIONS

7.1 Effect of pressure (varying back pressure plates).

The effect of pressure has been studied in previous experimental work. In pure water solutions. and in $NaCl-H_2O$ solutions, the solubility of anhydrire is significantly affected by large pressure differences (about 500 bars) (Dickson et al.. 1963: Blount and Dickson. 1969). In normal geothermal production, the pressure inside the wellbore can only be varied over a very limited range through the use of back pressure plates: for exampie from 6 to about 20 bars for CN-I. Anhydrire solubility is not significantly affected over rhis pressure interval (Blount and Dickson. 1969). as shown in Figure 2 and Appendix 1. In actual operations, varying pressure plates will probably affect anhydrite saturation through changes in the interplay of the various production zones of the well which involve changes in sulfate concentration and temperature between zones. In CN-1. for exampie. discharge fluid at BPP B4 during the baseline stage yielded the lowest concentration of sulfate. and the most pronounced undersaturation condition wirh respect to anhydrite (Figure 3b). The reduction in the anhyarire solubility product is probably caused by the prevalence of' a fluid from a different feed zone rather than the increase in pressure.

7.2 Effect of pH

Figure 13 shows the effect of pH change on anhydrite solubility and on the activities of sulfate and calcium species. The SOLVEQ program (Reed and Spycher, 1990a) which has an option for changing pH is used to simulate consequences of pH increase and decrease. Lowering the pH, i.e. increasing the molar concentration of hydrogen ions revealed a significant effect on anhydrite supersaturation. Decreasing deep water pH from the original values of 6.12 and 6.39 for CN-1 and CN-3D respectively, to pH 5.0 resulted in normal saturation and eventually in undersaturation as pH is lowered continuously. The effect of lowered pH is a decrease in $SO_4^{=}$ activity and a corresponding increase in HSO_4^- activity. Formation of bisulfate ion is favored at high

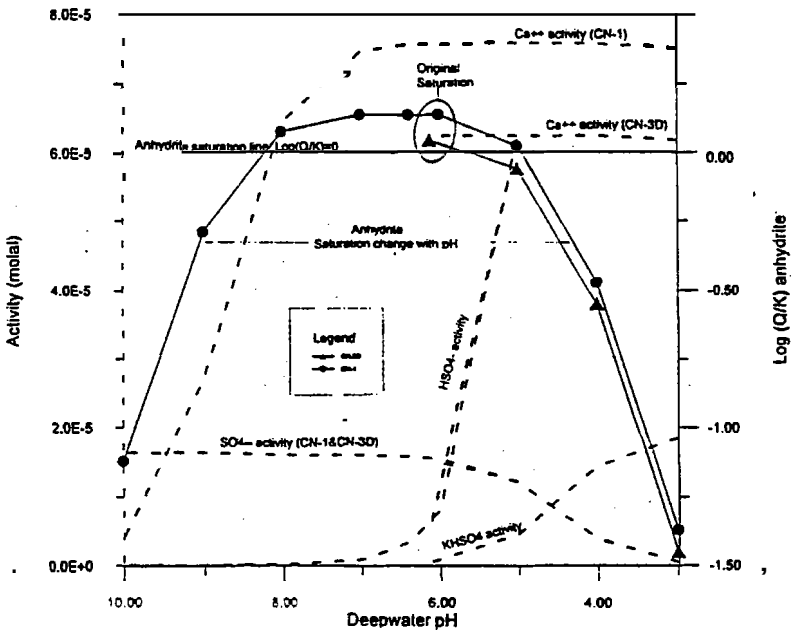

FIGURE 13: Effect of pH on anhydrite saturation, and calcium and sulfate activity at 270°C. pH changes are simulated using the SOLVEQ program with samples from CN-1 and CN-3D supersaturated with anhydrite.

hydrogen ion activity (low pH) as shown by the reaction,

$$SO_4^{--} + H^+ \rightarrow HSO_4^- \qquad (7)$$

where increase in H^+ activity will shift reaction to the right. The activity of KHSO, also increased as some bisulfate associates with potassium ions (K^+). The lower sulfate activity results in a lower anhydrite activity product as calcium activity remains constant while pH is decreased. This pH effect shows that in CN-1 and CN-3D, the pH of the mixture from which anhydrite is deposited is probably near neutral despite the low pH of the mixing fluids. At pH above 8, the anhydrite activity product will also decrease as calcium will be consumed by the formation of calcite, and other associated calcium species'.

7.3 Effect of temperature

As menrioned eariier. the effect of temperature on anhydrite solubiiity has been studied experimentally by Dickson et al. (1963) and Blount 2nd Dickson. (1969). Both SOLVEQ and WATCH have options

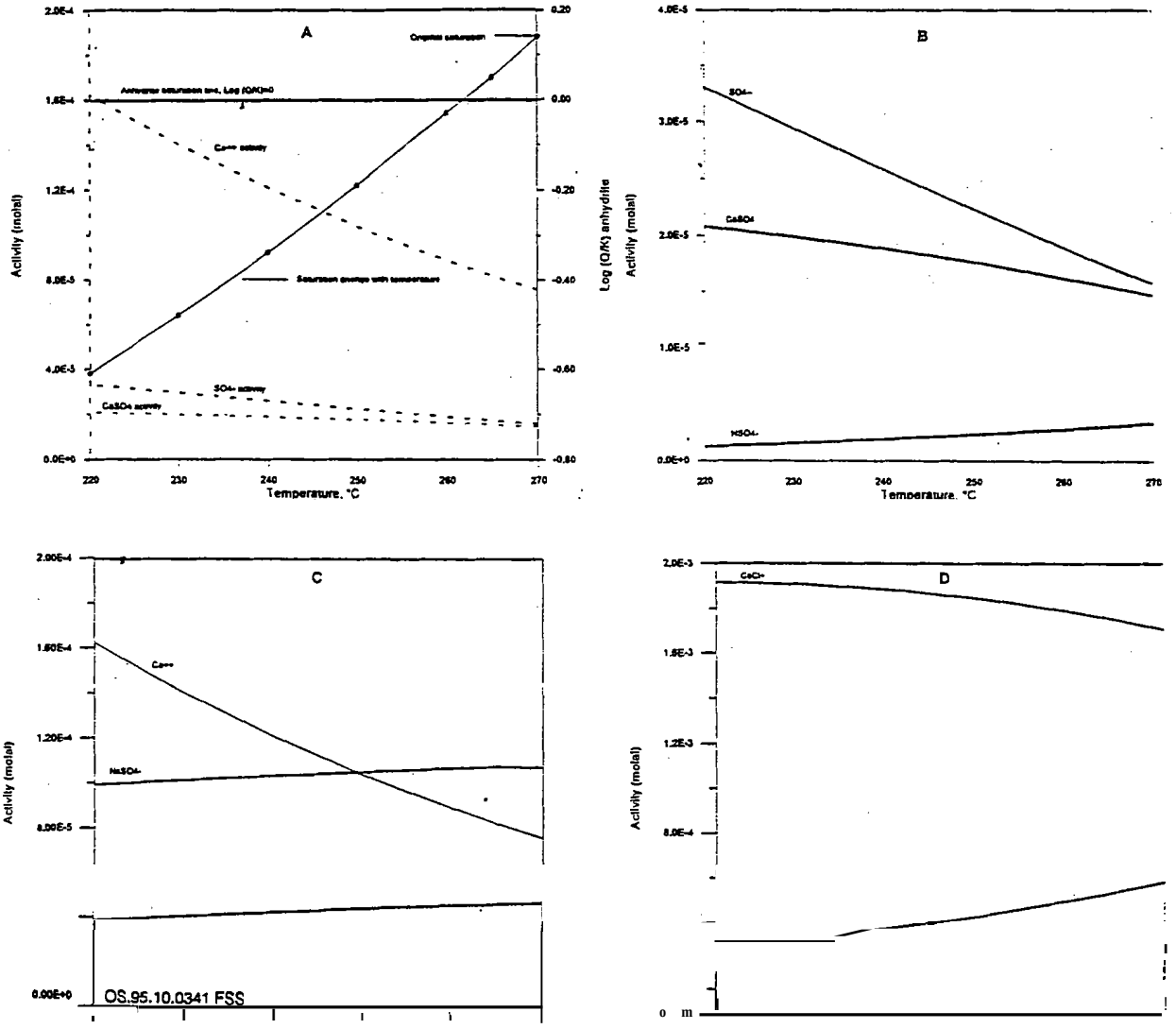

for cooling and heating. Simulation runs with these programs show that indeed as temperature decreases, the activities of calcium and sulfate ions increase, i.e. the solubility of anhydrite increases and undersaturation is approached (Figure 14). Thus at lower temperatures more anhydrite can be dissolved and the tendency to deposit is lower. This is supported by the higher thermodynamic equilibrium constants for anhydrite at lower temperatures. In CN-1, a 10°C drop in temperamre will result in undersaturation.

Figure 14 also shows the effect of temperamre on calcium and sulfate species. The activities of sulfate species such as $NaSO_4^-$, KSO_4^-, and HSO_4^- increased slightly with temperature indicating that these species become more associated with sulfate ions at higher temperature. However this increase in association is not enough to offset the decrease in solubility of sulfate at higher temperature and prevent theprecipitationofanhydrite.Calciumchloride ($CaCl_2$) also exhibited increase with temperature indicating more association of calcium and chloride ions. These temperature-speciation results imply that if these associations at higher temperatures of sulfate and calcium ions with Na^+, K^+, H^+, and Cl^- ions can be enhanced, the tendency for anhyarite to deposit will be reduced.

7.3 Effect of NaCl addition

The effect of NaCl on anhydrite solubility at different pressure and temperature has been investigated by Blount and Dickson, (1969). Their experimental conditions covered wide ranges of temperamre ana pressure and their results have shown that anhydrite is more soluble in NaCl solution than in pure H_2O. Their experiments, however, were conducted in a NaCl-H_2O-anhydrite solution in which the chemical matrix is very different from that of a geothermal brine such as that ofthe Cawayan wells.

The **CHILLER** program is used to simulate the effect of NaCl addition to the supersaturated fluid from well CN-I. One kilogram of CN-1 fluid is titrated with 0.01 to 0.10 fractions of one mole NaCl at 270 °C. The result (Figure 15) shows that NaCl apparently dissolves the anhydrite deposit, and converts the fluid from supersamrated to undersaturated condition. Initially the fluid is depositing approximately 0.016 g of anhydrite. Upon addition of NaCl, the amount of deposit is reduced significantly. When a fraction of 0.04 has been added, deposition stops and the solution starts to become undersaturated with respect to anhydrite.

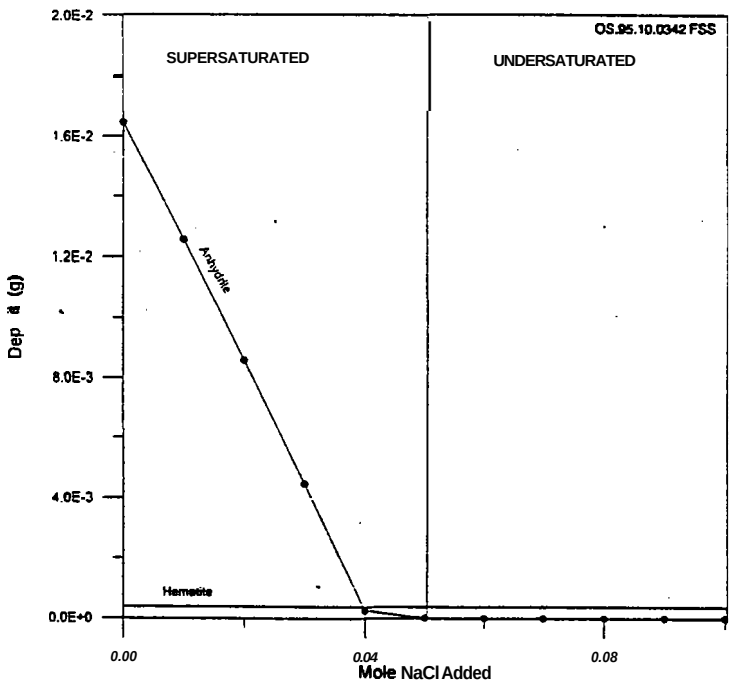

FIGURE 15: Effect of NaCl addition on annydrite deposition. Initial deposition at anhydrite supersaturation is approximately 0.16E-0 1g/kg solution. Addition of NaCl significantly reduces amount of deposit; at 0.05 mole NaCl added, deposition of anhydrite stopped, and normal saturation is attained. Further addition of NaCl resulted in undersaturation. Hematite is deposited but on a much smaller scale. Simulation is carried out using CHILLER with a sample from CN-1, supersaturated with anhydrite, at 270°C.

Figure 16 shows the effect of NaCl addition on the calcium and sulfate species of the supersarurated fluid. Evaluation of these species during the titration process showed that the most probable cause of undersaturation with respect to anhydrite is the significant decrease in calcium activity, and the

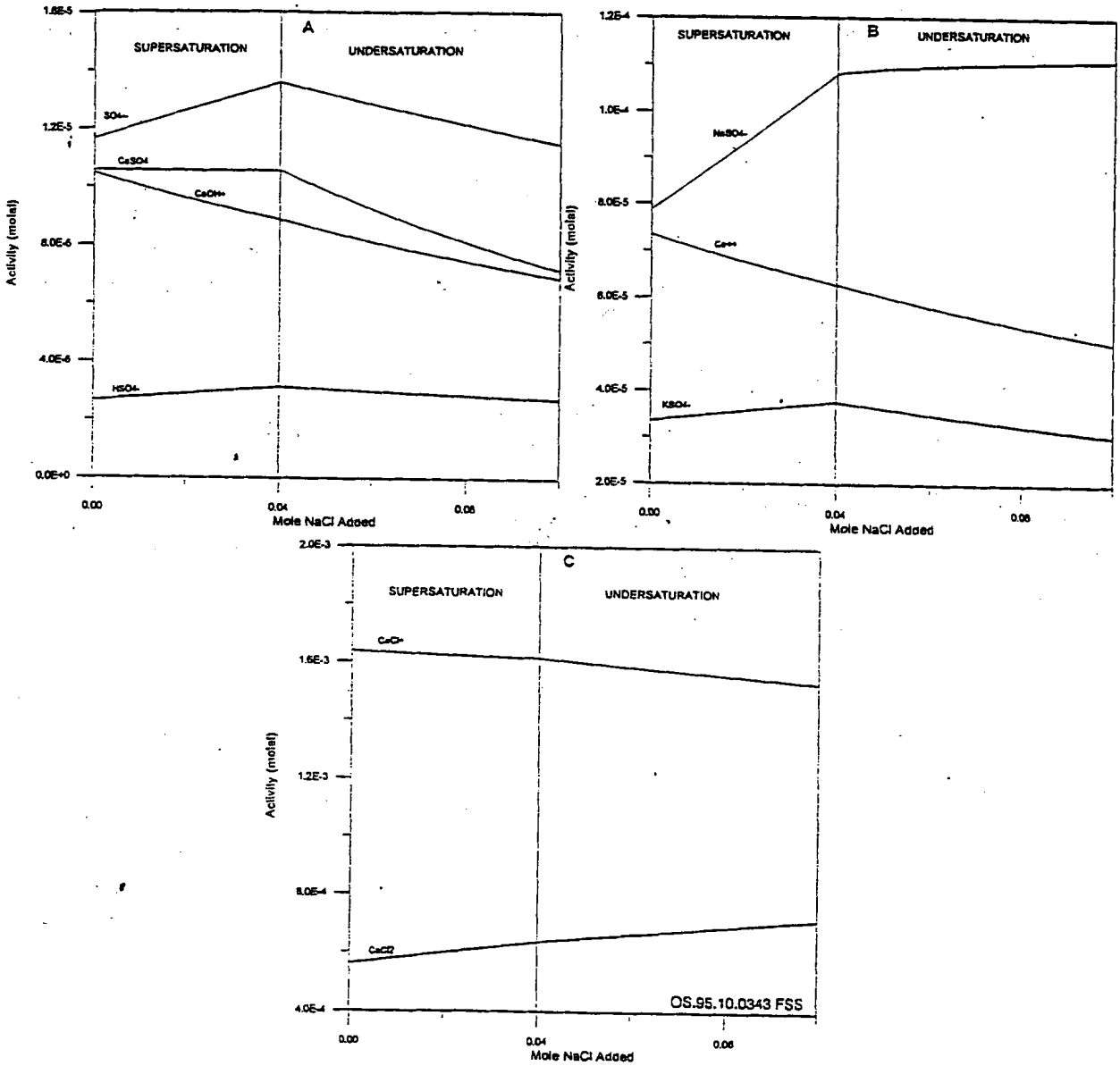

FIGURE 16: Effect of NaCl addition on calcium and sulfate species at 270 °C. Simulated titration using the **CHILLER** program with CN-1 fluid supersaturated with anhydrite.

significant increase in $NaSO_4^-$ activity. Sulfate at first, exhibited an increase in activity during Titration at anhydrite supersaturation because of the apparent dissolution of anhydrire. Initially, both sulfate and calcium are present in the solid phase as anhydrite mineral; upon addition of NaCl, these ions apparently dissolve and rejoin the liquid phase. A significant amount of the redissolved sulfate associates with sodium ion to form $NaSO_4^-$. Other sulfate species such as KSO_4^- and HSO_4^- aiso exhibited slight increases in activity, but these associations are apparently not sufficient to consume all the redissolved sulfate. Thus some sulfate-exists as free SO_4^{--} as shown by the increase in its activiry during titration at anhydrite supersaturation. Calcium ion activity exhibited a steady decline despite the dissolution because of its association with chloride as CaCl, which increased significantly, probably

enough to consume all the redissoived calcium species. After normal saturation is attained, sulfate and calcium activities declines continuously with increased NaCl addition. The decrease in the activiry of these two ions at constant temperature implies lower log Q and less tendency to deposit anhydrite. $NaSO_4^-$ and CaCI, activities continue to increase. Apparently, the effect of NaCl addition is to associate sulfate ion as $NaSO_4^-$ and calcium ion as $CaCl_2$ and thus significantly decrease the activity of unassociated calcium and sulfate ions which are responsible for anhydrite supersaturation and eventually, deposition.

8.0 INDUCED DEPOSITION: CaCl, INJECTION

The concept of inducing deposition of anhydrite in acid zones by the addition of "excess" calcium and thus forming a "barrier", seal-off acid fluids. and protect the casings, has been discussed in several PNOC-EDC internal reports, and has actually been pracriced during drilling.

The CHILLER program fluid-fluid mixing option is utilized to simuiate the mixing of high-sulfate acid fluid with CaCl, at different temperatures and mixing proportions. The purpose is to find out whether deposition is indeed induced and whether sulfate is removed from rhe solution.

Figures 17 and 18 show the effect o f CaCI, addition on anhydrite deposition and on the activity of sulfate ions at different temperatures. The simulated

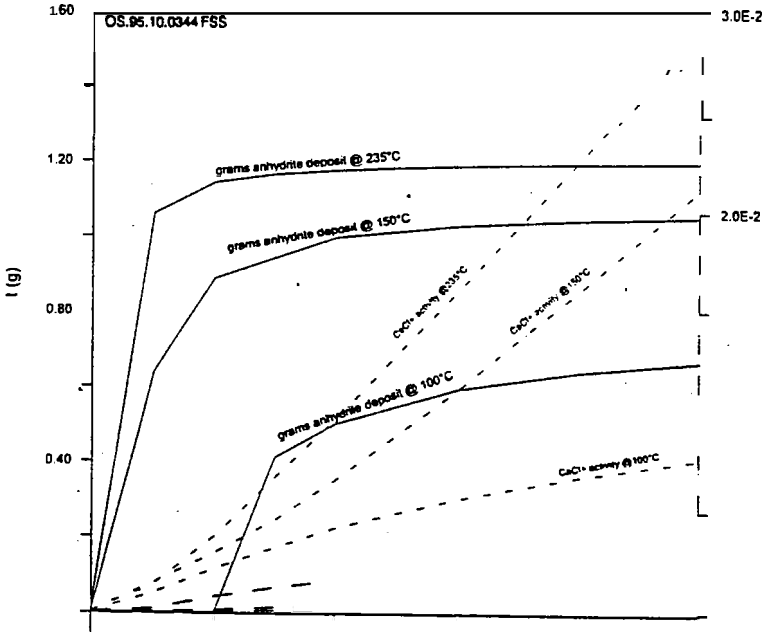

CaCI, addition also has significant effects on the various sulfate species (Figure 19). In its natural condition at the assumed temperature of 235°C, the acid-sulfate water contains bisulfate (HSO_4^-) as the niajor sulfate species followed by $NaSO_4^-$, SO_4^{--}, and KSO_4^-. Other species such as $MgSO_4$, $FeSO_4$, and $KHSO_4$ also exist in significant amounts. Addition of CaCl, drastically reduces the activities of these species as sulfate is consumed by the induced deposition of anhydrite. The hydrogen ion activity however increases, i.e. pH decreases and the fluid becomes more acid as CaCl, is added. The dissociation of bisulfate probably controls the pH of the mixture according to reaction (7). As more calcium is added, more sulfate is removed thus shifting the reaction to the left favoring the formation of more hydrogen ions. Such a reaction may have adverse effects since the fluid becomes more corrosive as the pH decreases. The simulated mixing showed that downhole pH declines from 4.86 to 3.42 as the fraction of CaCl, added is increased from 0.01 to 0.02 (Figure 19).

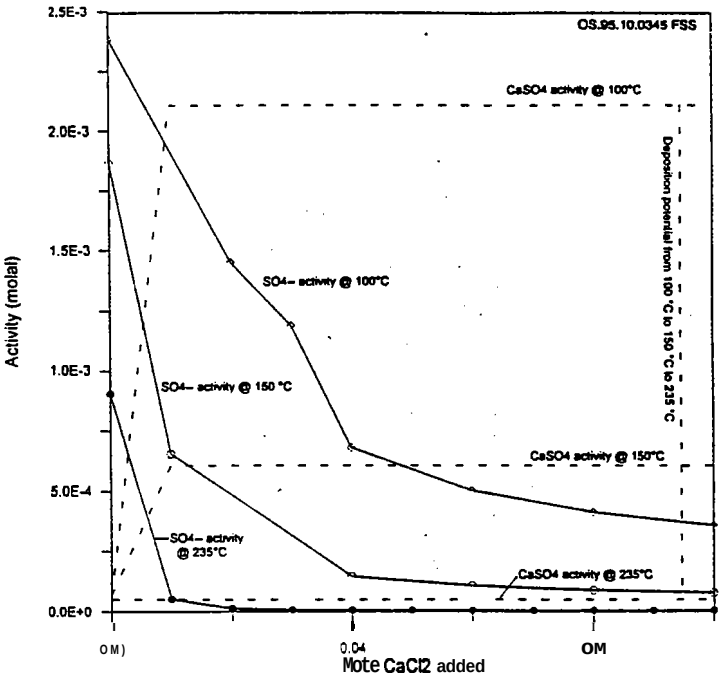

FIGURE 18: Effect of CaCI, addition on $CaSO_4$ and sulfate ion activities of high-sulfate acid downhole water from CN-1 at different temperatutes. Simulated mixing carried out using **CHILLER** program.

and that temperature plays a very critical role in this injection scheme. Since the $CaCl_2$ injectare is usually pumped at low temperature, the injection zone temperature must be high enough and the heat recovery fast for the injection to be effective. Otherwise the addition of $CaCl_2$ will only increase the potential of the fluid to deposit anhydrite especially when it comes into contact with a hotter fluid. Deposited anhydrite in the formation rocks also has the tendency to be dissolved at colder temperatures, and be redeposited at higher temperatures. Calcium chloride injection also tends to lower the downhole pH. This method, although it can probably induce "beneficial" deposition, has apparently some harmful consequences and therefore needs further evaluation in future applications.

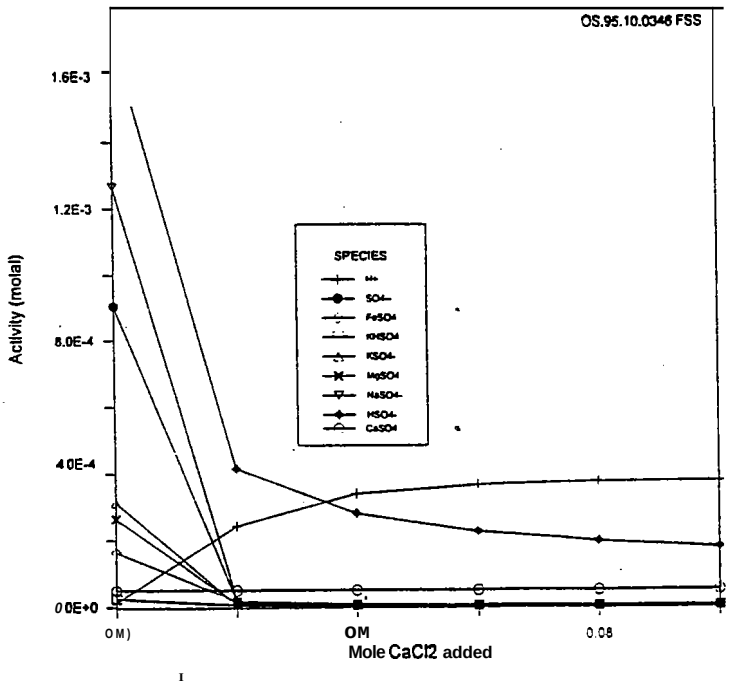

FIGURE 19: Effect of $CaCl_2$ addition at 235°C on calcium and sulfate species, and hydrogen ion activity of CN-1 high-sulfate acidic downhole water.

9.0 POSSIBLE METHODS OF CONTROL

9.1 NaCl / Na_2HPO_4 addition

Both experimental studies and simulation runs have shown that NaCl can significantly increase the solubility of anhydrite in solution thus decreasing its potential for deposition. In the Cawayan field the problem of anhydrite deposition is mainly caused by the acid fluid that corrodes the casing and permits the entry of the high-sulfate fluid. Treatment with NaCl will not solve the corrosion problem; however, it can prolong the life of the well by retarding deposition.

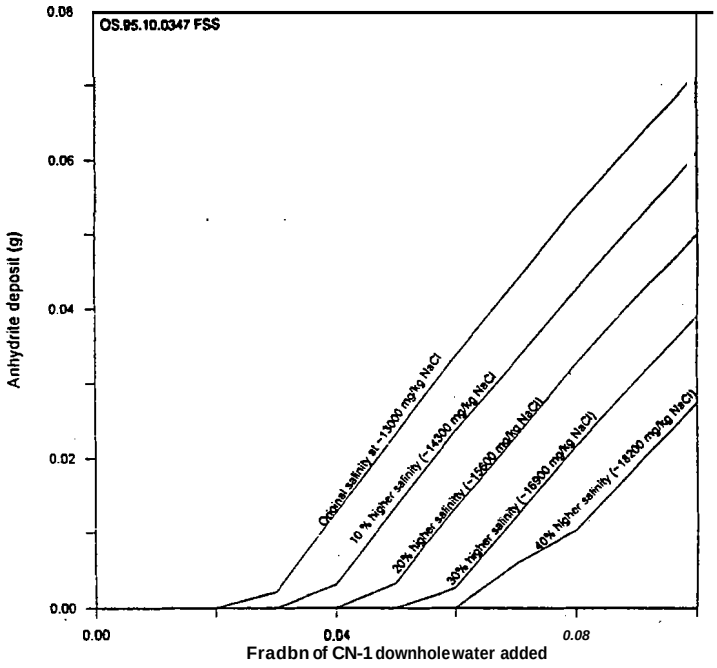

FIGURE 20: Effect of increasing salinity (NaCl concentration) on anhydrite deposition from CN-1 production fluid ar **270°C** and different fractions of high-sulfate downhole fluid.

Figure 20 shows simulated increases in the salinity of well CN-1 fluid and the effect of increasing the amohnt of mixing fluid on anhydrite deposition. The salinities are increased by 10, 20, 30, and 40% of the original NaCl concentration prior to mixing with different amounts of CN-1 high-sulfare downhole fluid. Results show that as the amount of NaCl is increased, the amount. of anhydrite deposit is significantly decreased. The fraction of the downhole fluid required to initiate deposition is also increased.

Injection with NaCl in the acid zones during

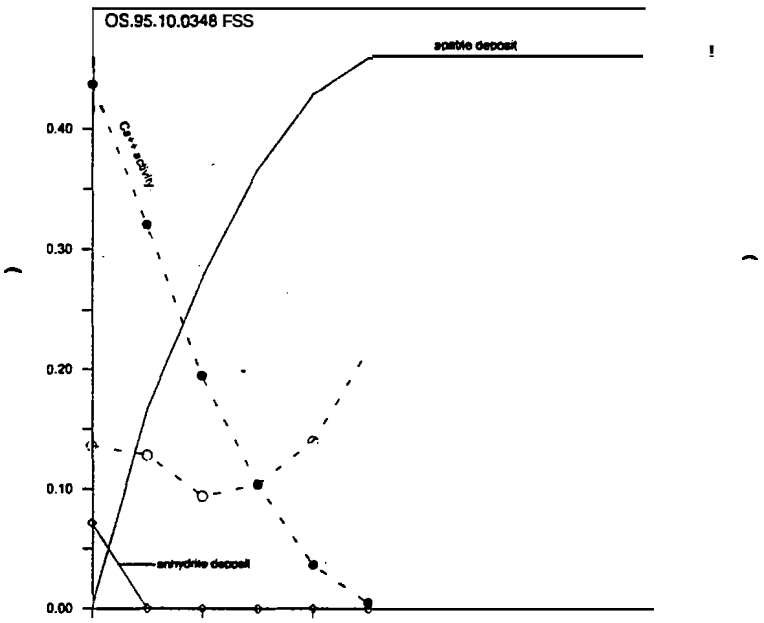

form apatite,

deposirion of apatite may take place as indicated by the simularion run.

9.2 pH reduction (acid injection)

Acid treatment is aiso a possible method of control. Although the main cause of deposition in Cawayan wells is acid fluid, the simularion runs have shown that the fraction of this acid fluid necessary for deposition is so small that it does not significantly affect the pH of the solution. Results of mixing simulation in CN-1 show that from an original downhole pH of 6.61, the mixed fluid pH decreased to only 5.62 after a 0.10 fracrion of the acid fluid had been added.

The effect of aciaificarion has been simuiated using CN-1 fluids mixed with 0.05 and 0.10 fractions of acidic high-sulfate downhole warer, titrated with 0.001 to 0.01 fractions of 0.01 mole of HCl after deposition has taken place. Figure 22 shows the results of the simulation runs. At the assumed 0.05 fraction of downhole water, all anhydrite deposit was successfully dissoived by a 0.005 mole fraction of HCl at pH 4.71. However at a higher fraction (0.10) of high-sulfate fluid mixed with the brine. the amount of HCl needed to approacn zero deposition is about 0.01 and this will reduce the. pH to 4.40. The caicuiared downhole pHs at 270°C can aiso decrease significantly at lower temperatures as more bisulfate ions . dissociate. But acid addition can be regulated, ana although deposition is not totally eliminated, it can be significantly reduced.

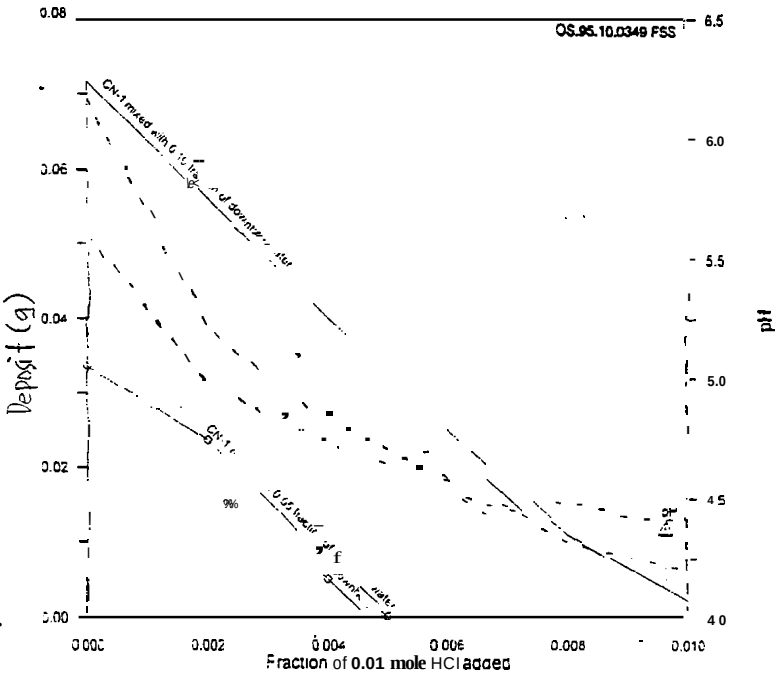

FIGURE 22: Effect of addition of 0.0 1 mole HCI on anhydrite deposition of CN-1 production fluid mixed with 0.05 and 0.10 mole of high-sulfate acid downhoie fluid. at 270°C.

9.3 Syntheric chemical additives

The effect of synthetic chemical additives on the morphology of calcium sulfate precipitated from seawater at 120-150°C has been inveaigated by Austin, et al. (1975). The results show that additives can displace SO_4^- and attach themselves to the Ca^- probably by O H bonding on the growth surface; identified effecrive additives contain PO_3H^- and CO_2H. This experiment was however conducted at relatively low temperatures.

Experimental studies for possible application in oil fields by Vetter (1970.)'showed that pnosphonates can be effective inhibitors of anhydrite deposition at temperatures of about 350°F **(177°C).** No data however were avaiiabie for higher temperatures.

Other possible synthetic chemical addirives are the NADAR Dispersants manufactured commercially by Nadar Chimica. These additives have mainly dispersant action and some complexing activity towards

calcium salts in saline environment (Prinetti, A., pers. comm.).

10.0 SUMMARY AND CONCLUSIONS

The anhydrite deposition in Cawayan wells is basically controlled by three factors: high-sulfate acid fluid, calcium-rich geothermal brine, and a high temperature of mixing. Mixing simulations and geochemical evidences suggest that the anhydrite deposit is an end-product of mixing between high-sulfate acid fluid and calcium-rich geothermal brine. Geochemical parameters such as sulfate, calcium, magnesium, chloride, and silica are effective indicators of deposition. The speciation programs WATCH and SOLVEQ can be used to monitor the anhydrite saturation of the fluids.

The reaction path program CHILLER can be an effective tool in predicting and possibly quantifying the rate and amount of anhydrite deposition. Preliminary results of simulation runs suggest that in the complex geochemical mamx of the Cawayan well fluids, the behavior of calcium and sulfate species can be manipulated by chemical addition such that the tendency for anhydrite deposition can be significantly reduced. Possible inhibitors screened by simulations include NaCl, Na_2HPO_4, and HCl. However, as mentioned earlier, there are always limitations to chemical equilibrium computations; one of which is "kinetic barriers" (Nordstrom and Munoz, 1986). Other factors in deposition process which may not be simulated by reaction path programs includes the effect of fluid velocity, thermal stability of some chemical inhibitors, nucleation and crystal formation, and adherence.of deposits. Therefore, pilot scale experimental studies are necessary for validation.

ACKNOWLEDGEMENT

I wish to convey my sincerest thanks to the government of Iceland, the United Nations University, PNOC-EDC, Dr. Ingvar Fridleifsson, Ludvik Georgsson, Susanna and Margret Westlund, my adviser Dr. Halldor Armannsson, Dr. Stefan Amorsson, the Orkustofnun lecturers and staff, and the UNU fellows of 1995.

REFERENCES

Amorsson, S., Sigurdsson, S., and Svavarsson, H., 1982: The chemistry of geothermal waters in Iceland I. Calculation of aqueous speciation from 0° to 370°C. *Geochim. Cosmochim. Acta, 46, 1513-1532.*

Austin, A.E., Miller, J.F., Vaughan, D.A., and Kircher, J.F., 1975: Chemical additives for calcium sulfate control. *Desalination, 16, 345-357.*

Bjarnasòn, J.O., 1994: *The speciation programme* WATCH, version 2.1. Orkustofnun, Reykjavik, 7 p.

Blount, C.W., and Dickson, F.W., 1969: The solubility of anhydrite ($CaSO_4$) in $NaCl-H_2O$ from 100 to 450°C and 1 to 1000 bars. *Geochim. Cosmochim. Acta, 33, 227-245.*

Dickson, F.W., Blount, C.W., and Tunell, G., 1963: Use of hydrothermal solution equipment to determine the solubility of anhydrite in water from 100°C to 275°C and from 1 bar to 1000 bars pressure.

American Journal of Science, 261, 61-78.

Fragara, J.F., **1991:** *Well CN-3D geology report.* PNOC-EDC Internal Report, 26 p.

Fragata. J.F., **1994:** *Well CN-4D* geology report. PNC-EDC Internal Report, **17** p.

Helgeson, H.C., **1969:** Thermodynamic of complex dissociation in aqueous solution at elevated temperatures and pressures. *Amer. J. Sci., 267, 729-804.*

KRTA (1983): *Summary of calcium sulfate solubility, controls and determination.* PNOC-EDC Internal Report, **1-53.**

KRTA **(1985):** *Acid sulphate fluids in the Bacon-Manito central reservoir.* PNOC-EDC Internal Report.

Nordstrom, D.K., and Munoz, J.L., **1986:** *Geochemical Thermodynamics.* Blackwell Scientific Publications, **427** p.

PNOC-EDC **(1989):** *Bacman II resource assessment.* PNOC-EDC Internal Report, **20-2**I.

Ramos, **S.G., 1991:** *Petrology of well CN-2RD.* PNOC-EDC Inrernal Report, 15 p.

Reed, M.H., and Spycher, N.F., 1990a: *User's guide for SOLVEQ: A computer program for computing aqueous-mineral-gas equilibria (revised preliminary edition), 36 p .*

Reed, **M.H.,** and Spycher, N.F., 1990b: *SOLTHERM: Data base for equilibrium consrants for aqueous -mineral-gas equililibria (preliminary and incomplete).* Depr. of Geological Sciences, University of Oregon, Eugene, Oregon, **47** p.

Reed, M.H., and Spycher, N.F., **1992:** *User's guide for CHILLER A program for computing water-rock reactions, boiling, mixing, and other reaction processes in aqueous-mineral-gas systems,* **64p.**

See, **F.S.,, 1991:** *Geochemistry of well CN-2RD.* PNOC-EDC Internal Report.

Solis, RP., **1988:** *Chemical signatures of the acidic fluids in the production wells of Bacon-Manito geothermal project.* PNOC-EDC Internal Report.

Solis, RP., Cabel, **A.C.,** See, **F.S.,** Candelaria, M.N.R., Buenviaje, M.M., **and** Garcia, S.E., **1994:** *Bacon-Manito geothermal production field pre-exploitation baseline geochemistry data* PNOC-EDC Internal Report, **94-97.**

Vetter, **O.J., 1972:** ***An*** evaluarion of scale of inhibitors. *J. Pet. Chem., (Aug. 1972), p. 997-1008.*

Vetter, **O.J.G.** and Phillips, R.C., **1970:** Prediction of deposition of calcium sulfate scale under downhole conditions. *J. Pet. Tech (Oct. 1970), 1299-1308.*

Yeatts, L.B., and Marshall, W.L., **1969:** Apparent invariance of activity coefficients of calcium sulfate at constant ionic strength and temperature in the system $CaSO_4$-Na_2SO_4-$NaNO_3$-H_2O to the critical temperature of water. *Association Equilibria. Journal of Physical Chemistry, 73, 81-92.*

TABLE 1 Cawayan representative baseline well discharge and downhole chemistry

WELL	DATE	BPP	WHP	Hd	TMF	SP	pH	Concentration in mg/kg *												mmole/100moles**	
			MPaa	kJ/kg	kg/s	MPaa	25°C	Na	K	Ca	Mg	Fe	Cl	SO4	H2S	HCO3	TCO2	B	SiO2	CO2	H2S
CN-1	09-12-81	A2	2.34	1220	38.3	0.094	7.78	4654	926	175	0.15		8757	23		10.7			873	229	6.92
CN-1	09-24-81	B1	2.43	1545	24.7	0.094	7.83	4784	950	169	0.13		8757	29		3.1		37	854	166	5.30
CN-1	09-29-81	FBD	0.84	1267	101.2	.094	7.73	4691	898	177	0.19		8686	26		7		36	865	175	5.25
CN-1	11-19-82	B4	0.09	1214	13	0.094	7.71	4542	921	174	0.06	0.23	8693	22		2.3		37	806	191	7.07
CN-2D	10-13-82	FBD	0.54	1174		0.507	3.83	2438	228	9	12.7	145	3425	1230	0.68			20	503	14844	54.6
CN-2D	10-20-82	FBD	0.53	1120		0.094	3.82	3111	291	13	16.2	179	4343	1610	0.35	150		23	608	16438	62.6
CN2RD	05-10-91	FBD	0.51	965	25.1	0.094	3.74	455	46	17	8.2	4.25	206	871				5	638	419	16.1
CN-3D	10-11-90	FBD	-	1232		0.728	7.24	4215	865	174	0.13	0.19	7768	25	2.52	13.4	12.3	41	741		
CN-3D	10-16-90	A1	2.44	1108		0.715	7.28	4215	899	171	1.39	1.08	7811	18		9.4	9.9	40	740	233	10.9
CN-3D	10-20-90	A3	2.2	1297		0.825	7.25	4150	886	173	0.15	0.17	7672	23		9.8	7.9	41	739	251	11.7
CN-4D	01-16-95	FBD	1.07	1222		0.839	7.05	3917	800	138	0.26	0.84	7031	19	4	10	9	33	742	286	11.0
CN3RD	09-13-91	FBD	0.35	922	19.6	0.094	8.89	400	25	7	1.39		276	382		75.1	12	6	527	489	10.6
DOWNHOLE SAMPLES (ACID FLUIDS)																					
		DEPTH,mVD																			
CN-1	09-04-89	SHUT	1500				3.2	1300	144	9	9.4	58.4	1713	884			49.3	14	572		
CN-1	09-0789	SHUT	800				3.8	1260	140	6	10.2	35.4	1615	810			22.9	15	557		
CN-1	09-18-89	SHUT	1400				3.4	1150	123	17.4	8.8	38.1	1590	975				16	592		
CN-1	09-19-89	SHUT	1550				4.1	1400	285	14.2	14.4	26.2	1948	827			10.6	15	533		
CN-3D	05-08-90	SHUT	1200				5.1	2600	554	89.4	1	28	4950	96				27	677		
CN2RD	06-19-91	SHUT	1775				2.9	575	37	11.3	4.2	44.2	177	894			4.3	4	356		
CN2RD	06-20-91	SHUT	1600				2.6	515	45	10.8	6.7	67.2	142	1056			37	4	466		
CN2RD	06-29-91	SHUT	1410				4.3	370	32.6	8.7	3.6	60.2	316	673			107	7	314		

* Total composition in water phase at sampling pressure (SP) // ** Total composition in steam phase at sampling pressure

Abbreviations: WHP - wellhead pressure // BPP - back pressure plate or orifice plate with different diameters // FBD - full-bore discharge // mVD - meters vertical depth
TMF - total mass flow // Hd - discharge enthalpy

TABLE 2: Cerro Prieto production representative discharge chemistry

WELL	DATE	BPP	WHP	Hd	SP	pH	Concentration in mg/kg *											millimoles/100moles		
			MPaa	kJ/kg	MPaa	25°C	Na	K	Ca	Mg	Fe	Cl	SO4	H2S	HCO3	TCO2	B	SiO2	CO2	H2S	NH3
CN-1	09-24-93	FBD	1.2	1216	0.094	.76	4581	897	226	0.25	0.39	8519	26		3.1	0.88	37	830	207	7.1	2
CN-1	11-09-93	FBD	0.96	1216	0.769	7.13	4140	722	196	0.21	0.27	7780	29		12.2	7.92	32	698	230	4.8	1.69
CN-1	01-03-94	FBD	0.94	1193	0.784	7.01	3981	629	186	0.29	0.27	6994	46		7.32	12.3	30	714	232	13.4	
CN-1	03-19-94	FBD	0.93	1214	0.728	6.92	3667	717	199	0.42	0.27	6649	55	0.8	12.8	11.5	28	701	257	6.9	
CN-1	04-03-94	FBD	0.94	1214	0.784	7.04	3453	621	196	0.38	0.39	6402	53	0.3	150		25	667	255	7.7	
CN-1	05-30-94	FBD	0.98	1122	0.797	6.35	3779	647	167	0.34	1.04	6854	50.1		9	6	29	690	200	11.2	
CN-1	06-29-94	FBD	0.91	1122	0.784	6.55	3509	654	171	0.47	0.29	6496	61		10	9	26	681	250	11	
CN-1	07-27-94	FBD	0.91	1212	0.772	6.73	3496	592	186	0.63		6175	60		12	10	25	640	288	14	
CN-1	08-29-94	FBD	0.81	1212	0.756	6.48	4485	563	170	0.72		5986	68		9	10	26	627	326	8.3	
CN-1	09-26-94	FBD	0.77	1322	0.728	6.55	3120	564	157	0.81	1.08	6099	60		8	6	24	616	312	8.6	
CN-1	10-28-94	FBD	0.8	1207	0.777	6.57	3424	561	159	0.66	0.17	5962	49		12	12	43	637	326	7.1	
CN-3D	12-13-93	FBD	1.06	1253	0.811	7.2	4431	879	182	0.13	0.4	7693	2.1		19.5	31.7	39	731	239	12.1	4.59
CN-3D	03-24-94	FBD	1.05	1227	0.834	7.32	4220	837	194	0.28	0.5	7597	34		14	12	39	722	188	9.20	
CN-3D	04-21-94	FBD	0.95	1232	0.832	7.1	4100	861	178	0.31	0.32	7626	35.8			7	38	730	173	7.00	
CN-3D	05-18-94	FBD	0.98	1232	0.839	6.95	4185	854	152	0.4	0.24	7542	42		15	11	38	726	205	12.2	2.89
CN-3D	06-17-94	FBD	0.94	1232	0.811	7	3941	848	158	0.57	0.35	7394	52		11	9	57	706	188	9.60	
CN-3D	07-21-94	FBD	0.96	1232	0.811	7.08	4017	819	158	0.83	0.2	7199	48		17	16	37	716	262	18.8	
CN-3D	08-17-94	FBD	0.92	1232	0.825	6.99	3655	832	150	0.93		7077	5.1		13	12	36	716	244	16.4	
CN-3D	09-20-94	FBD	0.84	1232	0.749	7.2	3783	786	137	1.29		6912	59		6	6	34	699	369	37.7	3.68
CN-3D	10-20-94	FBD	0.9	1190	0.804	6.93	3733	724	126	1.54		6483	54		16	12	33	684	247	9.40	
CN-3D	11-16-94	FBD	0.92	1222	0.804	7.03	3422	762	122	1.59		6581	58		9	7	26	777	204	12.3	
CN-3D	11-22-94	FBD	0.94	1222	0.811	6.88	3369	762	136	1.65		6803	52		10	7	34	727	211	9.80	
CN-3D	12-02-94	FBD	0.83	1222	0.804	7.16	3454	709	127	1.65		6348	52		7	2	32	665	214	11.6	
CN-3D	12-16-94	FBD	0.91	1222	0.784	6.86	3872	753	138	1.94		6739	60		16	3	35	711	215	8.70	
CN-3D	12-29-94	FBD	0.87	1222	0.804	6.57	3708	728	124	-		6544	62		-	-	33	689	208	9.00	
CN-3D	01-04-95	FBD	0.89	1251	0.804	6.94	3547	726	128	2.25		6411	66		6	6	32	602	204	9.00	
CN-3D	01-11-95	FBD	0.908	1251	0.811	6.76	3498	734	120	2.34		6284	6.1		8.5	8	3.1	681	240	9.00	
CN-4D	02-13-95	FBD	1.14	1216	0.874	6.96	3603	762	131	.17		6996	20		14	13	32	738	143	8.00	

* Total composition in water phase at sampling pressure (SP) // ** Total composition in steam phase at sampling pressure

TABLE 3: Mineral composition of wellbore **deposits**

DEPTH	DATE	COMPOSITION	%
WELL CN-1			
1599 mVD[a]	May 11, 1983	Corrosion products Anhydrite	90% 10%
1593 mVD[a]	May 28, 1984	Cuttings Corrosion products Anhydrite	60% 30% 10%
1598 mVD[a]	Sept. 19, 1984	Corrosion products cuttings Calcite Anhydrite	40% 30% 20% 10%
1383 mVD[b]	Feb. 21. 1990	Anhydrite Opaques - consist of : Pyrite 50% Pyrrhotite - 40% Hematite - 3% Magnetite - 2% Chalcopyrite - 2% Goethite - 3% Sphalerite - <1% Bornite - <1% Ilminite - <1% Gold <1% Vermiculite Cuttings (Dsp, I – Qn) Carbonates (Dol > ank >Ct)	46% 25% 15% 12% 2%
1019 mVD	May 24, 1994	Anhydrite Pyrite/hematite/magnetite/ goethite Cement Formation rock	79% 15% 3% 3%
WELL CN-3D			
1076 m MD[c]	Nov. 11, 1994	Anhydrite Pyrite	90% 10%
886 m MD	July 17, 1995	—no scraper sample—	--

[a] Petroanalysis by **A.G.** Reyes **and** E.L. Bueza, 1983-84
[b] Petroanalysis by A.G. Reyes, 1990
[c] Peuoanalysis by S.G. Ramos, 1994

TABLE 4: Comparison of different Log K values for annyanre

TEMP °C	BLOUNT AND DICKSON.1969 5 bars	55 bars	20 bars	ARNORSSSON 1869	YEATS AND MARSHALL.1869	Reed and Spycner, 1990
160	-6.613	-6.550	-6.590	-6.529	-6.345	-6.410
180	-7.075	-7.010	-7.050	-6.863	-6.701	-6.790
200	-7.538	-7.470	-7.520	-7.207	-7.072	-7.210
220	-8.000	-7.930	-7.980	-7.561	-7.457	-7.660
240	-8.463	-8.390	-8.440	-7.923	-7.856	-8.160
260	-8.925	-8.850	-8.850	-8.292	-8.270	-8.740
280	-9.388	-9.310	-9.310	-8.667	-8.697	-9.420
300	-9.850	-9.760	-9.760	-9.048	-9.138	-10.220

APPENDIX

Appendix I: Formulas used for calculating anhydrite solubility

1. Amorsson, et al, 1982

$$\log K = 6.20 - 0.0229T - \frac{1217}{T} \quad (°K)$$

2. Yeatts and Marshall, 1969 For solid-ion equilibrium

$$\log K_{isp} = -133.207 + 53.5472 \log T + \frac{3569.6}{T} - 0.0520925T \quad (°K)$$

3. Blount and Dickson, 1969

$$\log m_e = -2.917 - 0.02314t + 0.001179P + 6.02 \times 10^{-9} Pt^2 - 2.07 \times 10^{-7}P^2$$

where m is solubility of anhydrite in molal, t is temperature in "C, P is pressure in bars

4. Reed and Spycher, 1990b General equation form for all aq. species. gases, and minerals incorporated in SOLVEQ program

$$\log K(T) = A + B*T + C*T**2 + D*T**3 + E*T**4 \quad (T \text{ in } °C)$$

where *A, B. C, D, E* are regression coefficients; for *anhydrite = 1.0 Ca^{++} + 1.0 SO_4^{-}*
A=-0.40468E+01, B=-0.65771E-02, C=-0.10075E-03, D=-0.45922E-06, E=-0.92941E-09
log K values are -4.265(25°C), -4.580(50°C), -5.345(100°C), -6.216(150°C), -7.213(200°C), -8.439(250°C), -10.218(300°C), -14.022(350°C)

Appendix II: Sample calculation of anhydrite saturation (from CN-3D data, 10-11-90)

Webre conc. @ SP=7.3 bars / H_d= 1232 kj/kg : SO; = 25.0 mg/kg Ca^{++} = 174 mgkg
Activity coefficients at 273°C : SO_4^{-} = 0.09 Ca^{++} = 0.132
Species in deep water : SO; = 6.52 mg/kg Ca^{++} = 129.9 mg/kg
Activity in Deep Water : $a = \gamma_i * m_i$

$m\ SO_4^{--}$ = (6.52 mg/kg) / (96000mg/mole) = 6.792E-05 mole/kg
$a\ SO_4^{-}$ = 0.09. * 6.792E-05 mole/kg = 6.112E-06 mole/kg

$m\ Ca^{++}$ = (129.9 mg/kg) / (40080 mg/mole) = 3.184E-03 mole/kg
$a\ Ca^{++}$ = 0.132 * 3.241E-03 mole/kg = 4.203E-04 mole/kg

$Q_{CaSO4} = a_{SO4--} * a_{Ca++}$
= 6.112E-06 * 4.203E-04 = 2.569E-09
$\log Q_{CaSO4}$ = -8.590
$\log K_{CaSO4}$ = -8.582 at 273 "C (calculated from thermodynamic data)
$\log (Q/K)$ = -8.590 -(-8.528)
= -0.008 thus this fluid is very slightly undersaturated or in near equilibrium with anhydrite since the log ratio is practically zero *($\log Q = \log K$)*

Appendix III: Sample of CHILLER run input data

CN-1 Production Fluid (09-29-81) MIX WITH CN-1 Downhole fluid (09-04-89)
CHILLER- RUN

```
< erpc >< ph >< pfluid >< temp >< tempc ><volbox-l><rhofresh>< rhoroc >
 .1,000E-11  .00000 55.00000 270.00000  270.00000  .00000  .00000  .00000

<  sinc  ><  slim  ><  totmix  >
 0.010000000    0.1000000   .000000000

< enth >< senth >< denth >< totwat >< solmin ><  rm  >< aqgrm >< suprnt >
  .00000 . .00000  .00000 90.00000 .0000E+00  .00000 999.08765 .1000E-19

-----  c ifra ipun nloo iste lims looc ient itre idea ipsa incr incp mins neut
  0  3  0  2  70  0  I  0  0  0  0  1  0  0  0  0

 saq> < name >     c      mtot      ><      mtry      ><gamma >  <   comtot   >
    1 H+             .300600000E-04  .408183988E-06   .5104   .2138E-02
    2 H20            .984667000E+00  .100000000E+01   .9929   .995316E+00
    3 Cl-            .235011443E+00  .215929676E+00   .4902   .4616E-01
    4 SO4--          .270700000E-03  .921174811E-04   .0811   .9202E-02
    5 HCO3-          .289600000E-03  .239437435E-04   .5049   .1120E-02
    6 HS-            .524700000E-05  .143917094E-05   .4918   .000000E+00
    7 SiO2(aq)       .144000000E-01  .773939953E-02  1.0000   .9521E-02
    9 Ca++           .441600000E-02  .827521482E-03   .0726   .2246E-03
   10 Mg++           .781500000E-05  .228567365E-07   .0641   .3866E-03
   12 K+             .229700000E-01  .217242575E-01   .5095   .3683E-02
   13 Na+            .204000000E+00  .190058424E+00   .4918   .5655E-01
   11 Fe+            .000000000E+00  .000000000E+00           .1046E-02

< min  > < mintry 7

<nomox 7  <  wtpc  ><ppm?

<supnam>
diopside
quartz
chalcedo
talc
rhodonit
antigori
anthophy
chrysoti
cristoba
wollasto
tremo1it
Fe-actin
enstatit
andradit
cristo-a
hedenber
<dontfr>
```

Appendix IV: Sample of CHILLER run output

CN-1 *9-19-81* MIX WITH CS-1 DOWNHOLE 9-4-89
CHILLER

SPECIES	NO.	CHARGE	TOT.MOLES	MTRY	GAMMA	MIXING SOLUTION
H+	1	1.	.300460E-04	.40816E-06	.5104	.21380000E-02
H2O	2	0.	.54657E+02	.10000E+01	.9929	.55248250E+02
Cl-		-1.	.23501E+00	.21393E+00	.4902	.46160000E-01
SO4--		-2.	.27070E-03	.92117E-04	.0811	.92020000E-02
HCO3-	8	-1.	.28960E-03	.23944E-04	.5849	.11200000E-02
NA+		+1.	.52470E-05	.14392E-05	.4918	.00000000E+00
SiO2(aq)			.14480E-01	.77394E-02	1.0000	.95210000E-02
Ca++			.44160E-02	.82752E-03	.0726	.22460000E-03
Mg++			.78150E-05	.22857E-07	.0641	.38660000E-03
K+			.22970E-01	.21724E-01	.3095	.36830000E-02
Na+	11		.20400E+00	.19096E+00	.4918	.58540000E-01
Fe++	12		.00000E+00	.10000E-09	1.0000	.10460000E-02

CHARGE BALANCE FOR TOTAL MOLES = -.277555576E-16
MAX. DIFFERENCE ALLOWED = .23501144E-04
CHARGE BALANCE FOR THE MIXING SOLUTION = .1400E-05
MAX. DIFFERENCE ALLOWED = .2350E-04

THE FOLLOWING PARAMETERS WERE GIVEN:

ERPC =	.1000E-11	PH =	.0000	Pfluid =	55.0000
SLIM =	.10000E+00	TEMP =	270.0000	SIMC =	.1000E-01
TEMPC =	270.0000	TOTMIX=	.00000E+00	ENTH =	.0000
SENTH =	.0000	DENTH =	.0000	TOTWAT =	90.0000
SOLMIN=	.0000E+00	EH =	.0000	AQERR =	999.0877
SCPRNT=	.1000E-19	Vbox-1 =	.0000	Rhofrz =	.0000
Rhotrce=	.0000				

THE FOLLOWING OPTIONS WERE SELECTED:

C =	3	IFRAC =	0	IPUNCH =	1
ISTEP =	0	LINSCL =	1	LOGC =	0
ITREF =	0	IDEAL =	0	IPSAT =	1
INCP =	0	MIMSCL =	0	MEUT =	0

NLOOP = 70
IENTH = 0
INCREM= 0

GIVEN PRESSURE GRID. 1 T-P POINTS READ

OF THE DERIVED SPECIES LISTED BELOW, ONLY THOSE WITH MOLALITIES ABOVE .1000E-19 WILL APPEAR ON THE OUTPUT

SPECIES	NO.	CHARGE	LOG K(DISS)	SPECIES	NO.	CHARGE	LOG K(DISS)
CaCl+	13	1.	-1.3828	FeSO4	36	0	-4.5449
CaCl2	14	0.	-2.9515	H2 aq.	37	0.	0.8012
CaCO3	15	0	3.2801	KCl	38	0.	-.1157
CaHCO3+	16	1.	+1.1957	KHSO4	39	0.	-6.5465
CaOH+	17	1	-7.1977	KSO4-	40	-1.	-2.5532
CaSO4	18	0.	-4.0917	MgCl+	41	1.	-2.3825
CH4 aq.	19	0.	5.8684	MgCO3	42	0	5.7459
HCl	20	0.	-.7292	MgHCO3+	43	1.	-2.9719
CO3--	21	-2.	11.5147	MgOH+	44	1.	5.4736
HCO3	22	0.	-6.0493	MgSO4	45	0.	-4.8303
FeCl+	23	1.	-1.4322	NaCl	46	0.	-.2349
FeCl2	24	0.	-2.0800	NaCO3-	47	-1.	9.3564
FeCl3	25	1.	4.3179	NaHCO3	48	0.	-.5695
FeCl4-	26	1.	3.3536	NaNS	49	0.	-.9695
FeCl2+	27	1.	5.8700	NaOH	50	0.	10.8546
FeCl2	28	0	-.0486	Na2SO4-	51	-1.	-1.9122
FeCl4-	29	1.	.6149	O2 aq.	52	0.	32.6587
FeOH+	30	1.	6.9461	OH-	53	-1.	12.1205
Fe(OH)2	31	0.	12.6124	S--	54	-2.	15.0210
Fe(OH)3	32	0.	11.6134	H2S aq.	55	0.	-7.2937
Fe(OH)3-	33	-1.	21.5608	HSO4-	56	-1.	-5.7127
Fe(OH)4-	34	-1.	19.5408	H2SiO4--	57	-2.	22.4675
FeSO4+	35	1.	-1.1697	H3SiO4-	58	-1.	8.9429

FOR MIXED GASES (JSCLS=6), LOG K(HYDROL) = LOG (K*P)

MINERAL	NO.	LOG K(HYDROL)	TRIAL MOLES	MINERAL	NO.	LOG K(HYDROL)	TRIAL MOLES
H2O gas	1	.082	.0000E+00	greenal1	24	14.677	.0000E+00
CO2 gas	2	-8.107	.0000E+00	grunerit	27	16.255	.0000E+00
CH4 gas	3	6.944	.0000E+00	gypsum	28	-7.547	.0000E+00
H2 gas	4	5.870	.0000E+00	halite	29	.704	.0000E+00
H2S gas	5	-7.484	.0000E+00	hematite	30	5.429	.0000E+00
HCl gas	6	.086	.0000E+00	kaolinite	31	+8.180	.0000E+00
SO2 gas	7	+6.359	.0000E+00	kerolite	32	12.373	.0000E+00
S2 gas	8	-12.882	.0000E+00	lime	33	17.478	.0000E+00
O2 gas	9	30.229	.0000E+00	magnesit	34	+2.440	.0000E+00
akermani	10	21.668	.0000E+00	magn-hyd	35	4.527	.0000E+00
andyarit	11	+9.068	.0000E+00	magnetit	36	8.979	.0000E+00
aragonit	12	-1.467	.0000E+00	merwinit	37	33.817	.0000E+00
artanite	13	9.341	.0000E+00	monticel	38	13.939	.0000E+00
brucite	14	5.034	.3000E+02	nesqueho	39	13.280	.0000E+00
calcite	15	-1.580	.0000E+00	periclas	40	9.779	.0000E+00
camin25	16	+4.471	.0000E+00	portlan4	41	12.423	.0000E+00
camin75	17	-2.726	.0000E+00	pyrite	42	-20.181	.0000E+00
cristo-b	18	-1.695	.0000E+00	pyrrhoti	43	-6.354	.0000E+00
dolomite	19	+4.838	.0000E+00	pyrrhot:	44	-6.350	.0000E+00
dolo-ord	20	+4.839	5 active	sepiolit	45	+4.904	.0000E+00
dolo-dis	21	+4.262	.0000E+00	serpolit	46	16.796	.0000E+00
fayalite	22	6.564	.0000E+00	siderite	47	-4.154	.0000E+00
ferreal	23	2.246	.0000E+00	silic-am	48	-1.660	.0000E+00
forsteri	24	11.508	.0000E+00	sylvite	49	.831	.0000E+00
graphite	25	-2.310	.0000E+00	wimeneo*	50	3.208	.0000E+00

THE FOLLOWING MINERALS AND/OR GASES WITH IDENTICAL INDEX ARE IN SOLID SOLUTION:

H2O gas	6
CO2 gas	6
CH4 gas	6
H2 gas	6
H2S gas	6
HCl gas	6
SO2 gas	6
S2 gas	6
wimeneo*	6

CN-1 9-29-81 MIX WITH CN-1 DOWNHOLE 9-4-89
CHILLER

NUMBER OF LOOPS USED = 10 LOOP LIMIT = 70

CHARGE BALANCE FOR TOTAL MOLES = -.277555576E-16
MAX. DIFFERENCE ALLOWED = .23501144E-04

TEMPERATURE=270.0000 C. P(FLUID)= 55.00000 BARS MIXER FRACTION= .0000000
WATER: MOLES LIQ. = 54.6566 EQ. LIQ. = .9867E+00
MOLES TOTAL= 54.6571 EQ. TOTAL= .9867 ACTIVITY= .9929
STOICHIOMETRIC IONIC STRENGTH=.2442726E+00 OSMOTIC COEF.= .8230

TRUE IONIC STRENGTH=.21743001E+00

SPECIES(N)	MOLALITY	LOG MOLALITY	ACTIVITY	LOG ACTIVITY	GAMMA	LOG GAMMA
1 H+	.475777E-06	-6.3226	.247868E-06	-6.6147	.510323E+00	-.2922
2 H2O			.992931E+00	-.0031	.992822E+00	-.0031
3 Cl-	.215922E+00	-.6657	.105833E+00	-.9754	.490132E+00	-.3097
4 SO4--	.920000E-04	-4.0362	.274553E-05	-5.5275	.610375E-01	-1.0913
5 HCO3-	.208477E-04	-4.6805	.105035E-04	-4.9774	.504486E+00	-.2968
NA+	.2225E-05	-5.6788	.950322E-06	-6.0145	.491726E+00	-.3083
SiO2(aq)	.14487E-01	-1.8390	.14487E-01	-1.8390	.10000E+01	.0000
Ca++	.83022E-03	-3.0808	.60360E-04	-4.2290	.72583E-01	-1.1393
Mg++	.16123E-05	-5.7923	.10332E-06	-6.9858	.64047E-01	-1.1936
K+	.217255E-01	-1.6630	.21067E-01	-1.8560	.90941E+00	-.2929
Na+	.19087E+00	-.7211	.93468E-01	-1.0293	.49177E+00	-.3082
Fe++	.70395E-23	-22.1525	.46539E-24	-24.3322	.66106E-01	-1.1796
CaCl+	.30138E-02	-2.5212	.15398E-02	-2.8125	.51125E+00	-.2914
CaCl2	.60360E-03	-3.2193	.60360E-04	-3.2193	.10000E+01	.0000
CaCO3	.13719E-07	-7.8627	.13719E-07	-7.8627	.10000E+01	.0000
CaHCO3+	.30683E-05	-5.5130	.15789E-05	-5.8016	.51125E+00	-.2914
CaOH+	.30572E-04	-4.5147	.15630E-04	-4.8060	.51125E+00	-.2914
CaSO4	.55492E-05	-5.2558	.55492E-05	-5.2558	.10000E+01	.0000
CH4 aq.	.11488E-11	-11.9398	.11353E-11	-11.9082	.10754E+01	.0316
HCl	.13774E-06	-6.8609	.13774E-06	-6.8609	.10000E+01	.0000
CO3--	.17206E-08	-8.7643	.13266E-09	-9.8773	.77088E-01	-1.1130
HCO3	.26649E-03	-3.5743	.28657E-03	-3.5428	.10754E+01	.0316
H2 aq.	.35725E-05	-5.4470	.38418E-05	-5.4155	.10754E+01	.0316
KCl	.15427E-02	-2.8117	.15427E-02	-2.8117	.10000E+01	.0000
KHSO4	.70502E-07	-7.1518	.70502E-07	-7.1518	.10000E+01	.0000
KSO4-	.60173E-04	-4.2206	.29492E-04	-4.5301	.49012E+00	-.3097
MgCl+	.51637E-05	-5.2870	.26400E-05	-5.5786	.51125E+00	-.2914
MgCO3	.80469E-11	-11.0944	.80469E-11	-11.0944	.10000E+01	.0000
MgHCO3+	.19957E-04	-4.6999	.10203E-04	-4.9913	.51125E+00	-.2914
MgOH+	.11057E-05	-5.9563	.56531E-06	-6.2477	.51125E+00	-.2914
MgSO4	.52108E-07	-7.2831	.52108E-07	-7.2831	.10000E+01	.0000
NaCl	.16987E-01	-1.7699	.16987E-01	-1.7699	.10000E+01	.0000
NaCO3-	.36256E-08	-8.4406	.17770E-08	-8.7503	.49012E+00	-.3097
NaHCO3	.36543E-05	-5.4372	.36543E-05	-5.4372	.10000E+01	.0000
NaNS	.225548E-06	-6.6467	.22558E-06	-6.6467	.10000E+01	.0000
NaOH	.53419E-05	-5.2723	.53419E-05	-5.2723	.10000E+01	.0000
Na2SO4-	.13616E-03	-3.9343	.36935E-04	-4.2446	.49012E+00	-.3097
OH-	.66488E-04	-4.1773	.30384E-04	-4.5089	.66600E+00	-.3316
S--	.331022E-23	-23.4802	.25518E-24	-24.5932	.77088E-01	-1.1130
H2S aq.	.28875E-05	-5.5395	.31055E-05	-5.5079	.10754E+01	.0316
HSO4-	.18014E-05	-5.7444	.93203E-06	-6.0306	.51740E+00	-.2862
H2SiO4--	.15712E-01	-4.8791	.42577E-10	-10.0631	.77088E-01	-1.1130
H3SiO4-	.13490E-03	-3.8636	.67059E-04	-4.1735	.49012E+00	-.3097

CHARGE BALANCE FOR ALL SPECIES = .6441E-16

TOTAL FRACTION OF MIXING SOLUTION ADDED: .0000000

Solid products produced: Mass: .000000 grams Volume: .000000 CM3
Warning, mineral volume may be in error because some mineral densities were not supplied in SOLTHERM. See mineral list at top of output.

GAS COMPOSITION AT SATURATION (4 ITERATIONS):

TEMPERATURE. 270.0000 DEG.C.
SAT. PRESSURE. 54.3250 BARS

GAS	MOLE FRAC.	FNI	FUGACITY	PARTIAL P. (BARS)
H2O gas	.9996E+00	.8331	.4525E+02	.5430E+02
CO2 gas	.3402E-03	.9806	.1812E-01	.1848E-01
CH4 gas	.1849E-11	1.1751	.5713E-09	.6862E-09
H2 gas	.3256E-04	1.0199	.1804E-02	.1769E-02
H2S gas	.5209E-05	.9350	.2646E-03	.2830E-03
HCl gas	.3587E-08	1.0000	.1948E-06	.1948E-06
SO2 gas	.2510E-10	1.0000	.1363E-08	.1363E-08
S2 gas	.3255E-15	1.0000	.1768E-13	.1768E-13

NON-IDEAL MIXING WITH H2O CO2. CH4 GASES

The following gases and minerals are presently EXCLUDED from matrix (Note that gases and minerals with log(Q/K) less than -5 are not listed below.

GAS OR MINERAL	LOG K	LOG Q	LOG(Q/K)	LOG(Q/K)/S	AFFINITY	LOG FUGACITY
1 H2O gas	.08	.00	-.08	-.085	.21061E-03	1.654
2 CO2 gas	-8.11	-11.59	-1.48	-2.161	.86558E-04	-1.742
3 CH4 gas	6.94	-4.04	-10.91	-2.746	.27303E-05	-9.263
4 H2 gas	5.87	1.39	-4.48	-2.561	.11147E-05	-7.744
5 H2S gas	-7.48	-12.80	-5.32	-2.659	.13219E-04	-3.577
6 HCl gas	.86	-7.59	-8.45	-4.225	.21007E-05	-4.731
7 SO2 gas	-6.36	-16.97	-10.61	-2.828	.26364E-05	-8.865
8 S2 gas	-12.88	-28.37	-15.49	-2.384	.38512E-05	-13.752
9 O2 gas	30.23	-2.74	-32.91	-21.939	.81800E-05	-32.907
10 akermani	21.67	10.58	-1.09	-.978	.27155E-04	
11 annvarit	-9.07	-9.35	-.28	-.140	.69546E-03	
12 aragonit	-1.47	-2.58	-1.11	-.392	.12925E-04	
13 artanite	9.34	6.24	-3.10	-.359	.44651E-04	
14 brucite	5.03	6.24	-1.80	-.359	.44651E-04	
15 calcite	-1.58	-2.58	-1.00	-.334	.24529E-04	
16 cristo-b	-1.69	-1.84	-.14	-.144	.35864E-03	
19 dolomite	-4.84	-7.93	-3.09	-.516	.76888E-04	
20 dolo-ord	-4.84	-7.93	-3.09	-.515	.76863E-04	
21 dolo-dis	-4.26	-7.93	-3.67	-.611	.91183E-04	
24 forsteri	21.51	10.64	-.87	-.096	.21530E-04	
28 gypsum	-7.55	-9.35	-1.81	-.452	.44911E-04	
29 halite	.70	-2.00	-2.71	-1.354	.67335E-04	
32 kerolite	12.37	11.35	-1.02	-.081	.25135E-04	
34 magnesit	-1.44	-5.35	-2.91	-.969	.72239E-04	
37 merwinit	33.82	29.58	-4.23	-.235	.10527E-05	
38 monticel	13.94	13.41	-.53	-.059	.13201E-04	
40 periclas	9.78	6.24	-3.54	-.884	.87947E-04	
41 portland	12.43	9.00	-3.43	-.684	.85018E-04	
46 sepiolit	16.80	13.91	-2.89	-.100	.71821E-04	
48 silic-am	-1.64	-1.84	-.20	-.199	.49259E-03	
49 sylvite	.83	-1.93	-1.76	-1.881	.93537E-04	

Calculations done for 270.0000 DEG.C.; 55.0000 BARS

MIXER FRACTION: .000000

	TEMPERATURE	STOC.IONIC STRENGTH	HEAT PER MOLE
ACTUAL SOLUTION:	270.000	.24427E+00	65.722
MIXING SOLUTION:	270.000	.00000E+00	.000

FRACT. OF MIXING SOLUTION ADDED: .010000
RITHOL= .5525E+00 OLEMOL= .5490E+02

NEW HEAT: 65.722 NEW TEMPERATURE: 270.000

NEW MIXER FRACTION: .010000
RESULTING TEMPERATURE: 270.000DEG.C.

SOLIDS AND GASES CARRIED

CHARGE BALANCE CHECK AFTER FRACTIONATION OR TITRATION : TBAL = .1400E-07

CN-1 9-29-81 MIX WITH CN-1 DOWNHOLE 9-4-89
CHILLER

NUMBER OF LOOPS USED = 10 LOOP LIMIT = 70

CHARGE BALANCE FOR TOTAL MOLES = .140000000E-07
MAX. DIFFERENCE ALLOWED = .23547304E-04